nature materials

SUPPLEMENTARY INFORMATION

DOI: 10.1038/NMAT4219

A photoreversible protein-patterning approach for guiding stem cell fate in three-dimensional gels

Cole A. DeForest[*1,2] and David A. Tirrell*[*1]*

[1]Division of Chemistry and Chemical Engineering

California Institute of Technology

Pasadena, CA, USA

[2]Department of Chemical Engineering

University of Washington

Seattle, WA, USA

Supplementary Information

DOI: 10.1038/NMAT4219

General synthetic information

Unless otherwise noted, synthetic reagents were purchased from Sigma-Aldrich or VWR International and used without further purification. Distilled water was obtained from a Thermo Scientific Barnstead MegaPure MP-1 Glass Still. All reactions were performed under an inert argon atmosphere in flame- or oven-dried glassware and were stirred with a Teflon-coated magnetic spinbar unless stated otherwise. Organic liquid reagents were added to reaction vessels by syringe or *via* cannula transfer. Solvent was removed under reduced pressure with a Buchi Rotovapor R-200 equipped with a V-700 vacuum pump and V-800 vacuum controller. Products were further dried *in vacuo* with a Welch 1400 DuoSeal Belt-Drive high vacuum pump. Lyophilization was performed on a Millrock Technologies BT85 benchtop manifold freeze-dryer outfitted with an Oerlikon Leybold Vacuum Trivac E2 pump. Flash chromatography was performed using EMD Millipore Silica Gel 60 (230-400 mesh) following the general procedure by Still, *et al*[1]. Semi-preparative reversed-phase high-performance liquid chromatography (RP-HPLC) was performed on a DioneX ultimate 3000 equipped with a Kinetex 5µm XB-C18 250 x 4.6 mm preparatory C18 column and an automated fraction collector. Microwave-assisted peptide synthesis was performed on a CEM Corporation Liberty 1. High-resolution mass spectrometry (HRMS) data were obtained in the Caltech Mass Spectrometry Laboratory with the assistance of Naseem Torian and Dr. Mona Shahgholi. Fast atom bombardment (FAB) and electron impact (EI) mass spectrometry was performed on a JEOL JMS-600H mass spectrometer, while electrospray (ES) data were collected with a Waters LCT Premier XE instrument. Matrix-assisted laser desorption/ionization time of flight (MALDI-TOF) analysis was performed on an Applied Biosystems Voyager DE-PRO. ^{1}H and ^{13}C NMR spectra were recorded at room temperature on Varian Inova instruments (either 300 or 500 MHz) and are reported in ppm relative to tetramethylsilane (TMS, $\delta = 0$). Ultraviolet-visible spectrophotometry (UV-Vis) was performed on a Varian Cary 50 Bio spectrophotometer or a Tecan Safire[2] multi-detection microplate reader. Photochemical reactions were initiated with a Lumen Dynamics OmniCure S1500 Spot UV Curing system with an internal 365 nm band-pass filter, and light intensity was measured with a Cole-Parmer Instrument CO Radiometer (Series 9811-50, $\lambda = 365$ nm). Confocal microscopy was performed in the Caltech Biological Imaging Center on either a Zeiss LSM 510 Meta NLO equipped with a Coherent Chameleon multiphoton laser or a Zeiss LSM 710 Meta NLO. Fluorescence confocal microscopy data were rendered in 3D with Bitplane Imaris. Rheological analysis was performed on a TA Instruments ARES rheometer. FRAP experiments were performed on a Zeiss LSM 5 Exciter with the assistance of Peter Rapp and analyzed with MathWorks MATLAB. Biochemical gradients were created with the aid of a Harvard Apparatus PHD 2000 Syringe Pump. Mammalian cell culture was performed in a Baker Company SterilGARD e3 Class II Type A2 Biosafety Cabinet. Cells were maintained in a Model 2300 VWR Scientific Products Incubator kept at 37 ºC and 5% CO_2.

DOI: 10.1038/NMAT4219

Method S1 Synthesis of poly(ethylene glycol) tetra-bicyclononyne (PEG-tetraBCN)

BCN-OH was synthesized according to a known synthetic route.[2]

Synthesis of (1R,8S,9s,Z)-ethyl bicyclo[6.1.0]non-4-ene-9-carboxylate (endo) and (1R,8S,9r,Z)-ethyl bicyclo[6.1.0]non-4-ene-9-carboxylate (exo)

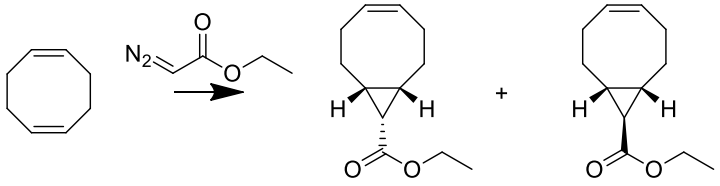

Ethyl diazoacetate (5.4 mL, 5.81 g, 51 mmol, 1x) in dichloromethane (30 mL) was added dropwise over 3 hrs to a flame-dried round bottom flask (500 mL) charged with 1,5-cyclooctadiene (50 mL, 44 g, 408 mmol, 8x) and rhodium(II) acetate dimer (1 g, 2.3 mmol, 0.045x) under argon at 0 ºC. After stirring at RT for 72 hrs, the mixture was filtered through silica and concentrated. The residue was purified by flash column chromatography (80:1 hexanes:EtOAc) to yield both the exo (5.12 g, 26.8 mmol) and the desired endo product (3.42 g, 17.6 mmol) in good yield (45% and 30%, respectively). *Exo*: ^{1}H NMR (500 MHz, $CDCl_3$) δ 5.68 – 5.56 (m, 2H), 4.08 (q, J = 7.1 Hz, 2H), 2.33 – 2.25 (m, 2H), 2.21 – 2.14 (m, 2H), 2.11 – 2.03 (m, 2H), 1.58 – 1.51 (m, 2H), 1.51 – 1.42 (m, 2H), 1.23 (t, J = 7.1 Hz, 3H), 1.17 (t, J = 4.6 Hz, 1H); ^{13}C NMR (126 MHz, $CDCl_3$) δ 174.53, 130.02, 60.35, 28.38, 27.98, 27.84, 26.76, 14.41; HRMS (EI+): calculated for $C_{12}H_{12}O_2^+$ $[M + {}^1H]^+$, 195.1385; found 195.1360 (Δ = -12.8 ppm). *Endo:* ^{1}H NMR (500 MHz, $CDCl_3$) δ 5.60 (ddt, J = 5.3, 3.5, 0.9 Hz, 2H), 4.11 (q, J = 7.1 Hz, 2H), 2.55 – 2.45 (m, 2H), 2.25 – 2.15 (m, 2H), 2.10 – 2.01 (m, 2H), 1.87 – 1.78 (m, 2H), 1.70 (t, J = 8.8 Hz, 1H), 1.43 – 1.34 (m, 2H), 1.26 (t, J = 7.1 Hz, 3H); ^{13}C NMR (126 MHz, $CDCl_3$) δ 172.44, 129.58, 59.86, 27.21, 24.32, 22.79, 21.38, 14.55; HRMS (EI+): calculated for $C_{12}H_{12}O_2^+$ $[M + {}^1H]^+$, 195.1385; found 195.1372 (Δ = -6.7 ppm).

Synthesis of (1R,8S,9s)-bicyclo[6.1.0]non-4-yn-9-ylmethanol (BCN-OH):

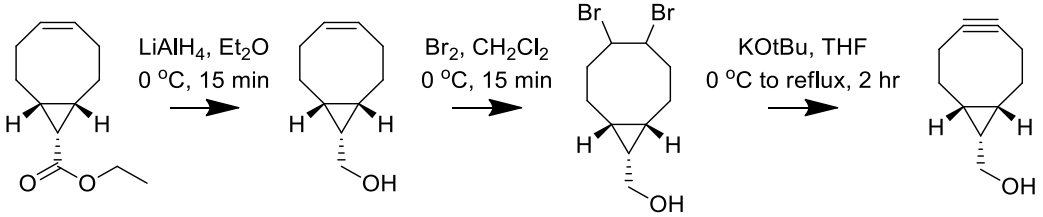

To a solution of endo intermediate (1*R,*8*S,*9*s,Z*)-ethyl bicyclo[6.1.0]non-4-ene-9-carboxylate 2.93 g, 15.1 mmol, 1x) in anhydrous diethyl ether (50 mL) was added dropwise a suspension of $LiAlH_4$ (590 mg, 15.6 mmol, 1.03x) in anhydrous diethyl ether (50 mL) at 0 ºC. The reaction was stirred at room temperature for 15 min before re-equilibration at 0 ºC, upon which minimal water was added until the grey solid turned white (4 mL). The mixture was dried over Na_2SO_4, filtered, and concentrated by rotary evaporation to yield the alcohol intermediate ((1*R,*8*S,*9*s,Z*)-bicyclo[6.1.0]non-4-en-9-ylmethanol).

A solution of Br_2 (1 mL) in anhydrous dichloromethane (15 mL) was added dropwise under an inert atmosphere at 0 ºC to a solution of the crude hydroxyl intermediate in anhydrous dichloromethane (115 mL) until a yellow color persisted. The reaction mixture was quenched

with aqueous sodium thiosulfate (10 wt%, 30 mL). After extraction into dichloromethane (3 x 60 mL), the combined organic layers were dried over Na_2SO_4, filtered, and concentrated *in vacuo* to yield the dibromide intermediate (((1*R*,8*S*,9*s*)-4,5-dibromobicyclo[6.1.0]nonan-9-yl)methanol).

The crude dibromide was dissolved in tetrahydrofuran (150 mL) under argon, and a solution of KOtBu (1 M in tetrahydrofuran, 50 mL, 50 mmol) was added dropwise to the flask at 0 ºC. The mixture was stirred under reflux for 2 hr (75 ºC) prior to quenching with saturated aqueous ammonium chloride (120 mL). The crude product was extracted into dichloromethane (3 x 60 mL), dried over $MgSO_4$, filtered, and concentrated under reduced pressure before purification by flash chromatography (4:1 hexanes:EtOAc). The purified product (BCN-OH, 1.56 g, 10.4 mmol) was isolated in excellent yield (65% over three steps). ^{1}H NMR (500 MHz, $CDCl_3$) δ 3.73 (d, J = 7.9 Hz, 2H), 2.36 – 2.16 (m, 6H), 1.67 – 1.54 (m, 2H), 1.34 (tt, J = 9.1, 7.9 Hz, 1H), 1.25 (s, 1H), 0.99 – 0.87 (m, 2H); ^{13}C NMR (126 MHz, $CDCl_3$) δ 99.02, 60.16, 29.19, 21.65, 21.56, 20.17; HRMS (EI+): calculated for $C_{10}H_{14}O^+$ $[M + {}^1H]^+$, 150.1045; found 150.1027 (Δ = -12 ppm).

Synthesis of (1R,8S,9s)-bicyclo[6.1.0]non-4-yn-9-ylmethyl (2,5-dioxopyrrolidin-1-yl) carbonate (BCN-OSu):

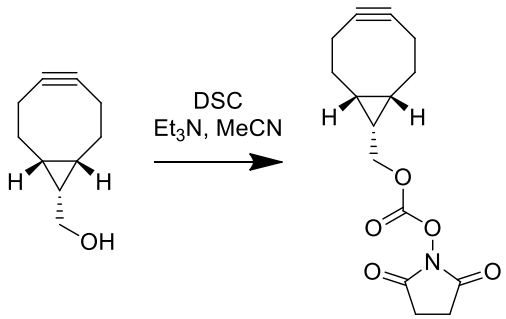

Triethylamine (4 mL, 2.92 g, 29.0 mmol, 3x) was added under argon to a solution of BCN-OH (1.45 g, 9.65 mmol, 1x) and *N,N'*-Disuccinimidyl carbonate (4.95 g, 19.3 mmol, 2x) in acetonitrile. The mixture was stirred overnight under an inert atmosphere, concentrated, and the residue was purified by flash column chromatography (3:1 hexanes:EtOAc) on silica gel. The pure product (BCN-OSu, 2.68 g, 9.20 mmol) was obtained in excellent yield (95%). ^{1}H NMR (500 MHz, $CDCl_3$) δ 4.44 (d, J = 8.4 Hz, 2H), 2.83 (s, 4H), 2.35 – 2.18 (m, 6H), 1.62 – 1.51 (m, 2H), 1.51 – 1.45 (m, 1H), 1.09 – 0.99 (m, 2H); ^{13}C NMR (126 MHz, $CDCl_3$) δ 168.83, 151.75, 98.81, 70.46, 29.08, 25.59, 21.43, 20.83, 17.29; HRMS (ES+): calculated for $C_{30}H_{34}N_2O_{10}Na^+$ $[2M + {}^{11}Na]^+$, 605.2111; found 605.2087 (Δ = -4 ppm).

DOI: 10.1038/NMAT4219

Synthesis of PEG-tetraBCN:

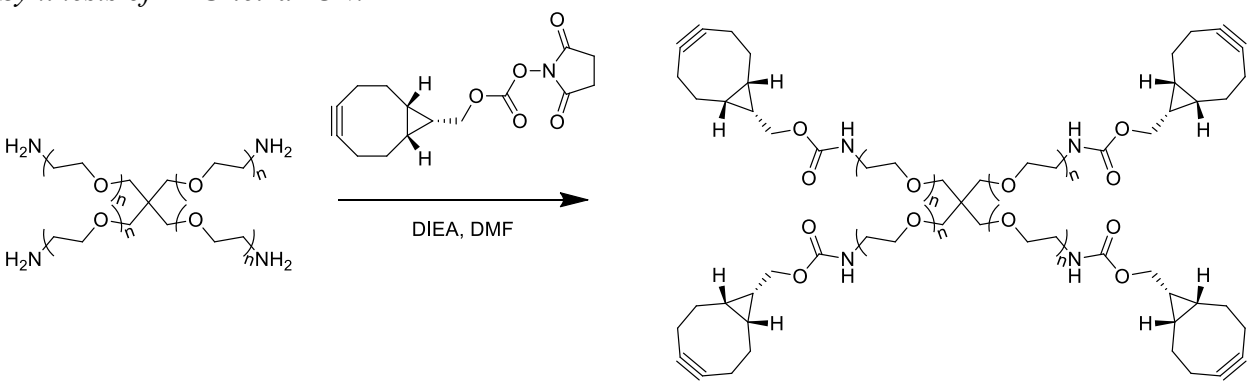

Four-arm poly(ethylene glycol) tetraamine (M_n ~ 10,000 Da, n ~ 57, 1 g, 0.4 mmol NH_2, 1x, Jenkem) and BCN-OSu (175 mg, 0.015 mmol, 1.5x) were dissolved in dimethylformamide (5 mL). *N*,*N*-Diisopropylethylamine (277 µL, 207 mg, 1.6 mmol, 4x) was added to the mixture, and the reaction was stirred overnight, concentrated, dissolved in water, dialyzed (molecular weight cutoff ~ 2 kDa, SpectraPor), and lyophilized to yield a white powder (1.06 g, quantitative yield). ^{1}H NMR (500 MHz, $CDCl_3$) δ 5.27 (s, 4H), 4.13 (d, J = 8.0 Hz, 8H), 3.78 – 3.75 (m, 8H), 3.65 – 3.61 (m, 909H), 3.50 – 3.47 (m, 4H), 2.30 – 2.18 (m, 24H), 1.64 – 1.50 (m, 8H), 1.39 – 1.29 (m, 4H), 0.98 – 0.88 (m, 8H). Functionalization was confirmed to be >95% by ^{1}H-NMR by comparing integral values for characteristic BCN peaks (δ 2.24, 1.57, 1.34, 0.92) with those from the PEG backbone (δ 3.63).

Method S2 Synthesis of MMP-degradable peptide crosslinker (N_3-DGPQGIWGQGDK(N_3)-NH_2)

4-azidobutanoic acid was synthesized according to a known synthetic route.[3]
Synthesis of ethyl 4-azidobutanoate:

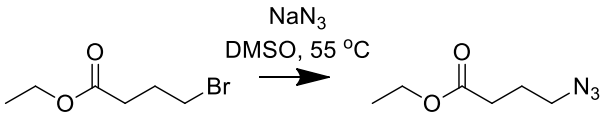

Ethyl-4-bromobutyrate (50 g, 256 mmol, 1x) and sodium azide (25 g, 384 mmol, 1.5x) were dissolved in dimethyl sulfoxide and stirred overnight at 55 ºC. The reaction mixture was diluted with water (250 mL) and extracted into diethyl ether (3 x 250 mL). The organic layer was washed with water (250 mL) and brine (250 mL), dried over $MgSO_4$, concentrated *in vacuo* to yield quantitatively the pure intermediate (39.5 g, 251 mmol) as a clear liquid. ^{1}H NMR (300 MHz, $CDCl_3$) δ 4.09 (q, J = 7.1 Hz, 2H), 3.31 (t, J = 6.7 Hz, 2H), 2.35 (t, J = 7.3 Hz, 2H), 1.86 (p, J = 6.9 Hz, 2H), 1.21 (t, J = 7.1 Hz, 3H); ^{13}C NMR (75 MHz, $CDCl_3$) δ 172.66, 60.54, 50.64, 31.16, 24.26, 14.19; HRMS (EI+): calculated for $C_6H_{12}N_3O_2^+$ [M + ^{1}H]$^+$, 158.0930; found 158.0901 (Δ = -18 ppm).

Synthesis of 4-azidobutanoic acid:

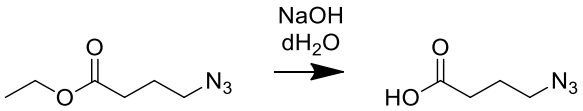

Ethyl 4-azidobutanoate (39.5 g, 251 mmol) was dissolved in aqueous sodium hydroxide (1 N, 250 mL). Methanol was added until the solution was homogenous (150 mL), and the mixture was stirred at room temperature for 3 hr. The methanol was removed under reduced pressure and the pH was brought to 0 with aqueous hydrochloric acid. The mixture was extracted into diethyl ether (3 x 250 mL), dried over $MgSO_4$, filtered, and concentrated *via* rotary evaporation. The clear liquid product (31.6 g, 245 mmol) was obtained in excellent yield (96%). ^{1}H NMR (500 MHz, $CDCl_3$) δ 10.61 (br s, 1H), 3.36 (t, J = 6.7 Hz, 2H), 2.45 (t, J = 7.2 Hz, 2H), 1.94 – 1.84 (m, 2H); ^{13}C NMR (126 MHz, $CDCl_3$) δ 179.19, 50.43, 30.92, 23.91; HRMS (FAB+): calculated for $C_4H_8N_3O_2^+$ [M + ^{1}H]$^+$, 130.0616; found 130.0598 (Δ = -14 ppm).

Synthesis of peptide crosslinker:
The base peptide H-DGPQGIWGQGDK(dde)-NH_2 was synthesized on rink amide resin (NovaBioChem) *via* standard microwave-assisted Fmoc solid phase methodology and HATU activation (CEM Liberty 1). The 1-(4,4-dimethyl-2,6-dioxacyclohexylidene)ethyl (dde) group was removed with 2% hydrazine monohydrate in dimethylformamide (3 x 10 min), and 4-azidobutanoic acid was coupled simultaneously to the N-terminal amine and the ε-amino group of the C-terminal lysine with HATU (Chem-Impex). Resin was treated with trifluoroacetic acid/triisopropylsilane/water (95:2.5:2.5) for 2 hr, and the crude peptide was precipitated in and washed (2x) with ice-cold diethyl ether. The crude peptide was purified using semi-preparative reversed-phase high-performance liquid chromatography (RP-HPLC) using a 40 min linear gradient (5–30% of acetonitrile and 0.1% trifluoroacetic acid) and lyophilized to give the product (N_3-DGPQGIWGQGDK(N_3)-NH_2) as a fluffy, yellow solid. Peptide purity was confirmed with

DOI: 10.1038/NMAT4219

analytical RP-HPLC and matrix-assisted laser desorption-ionization time-of-flight mass spectrometry using α-cyano-4-hydroxycinnamic acid matrix: MALDI-TOF: calculated for $C_{62}H_{92}N_{23}O_{20}^{+}$ $[M + {}^{1}H]^{+}$, 1478.7; found 1477.8.

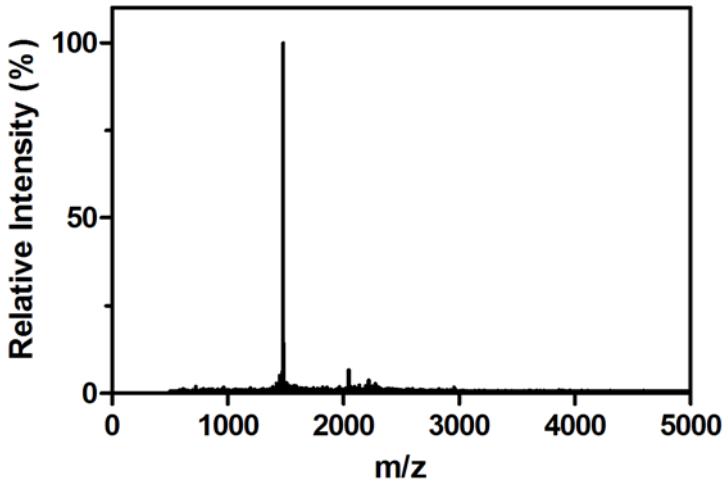

Method S3 Preparation of azide-functionalized glass slides

Synthesis of (3-azidopropyl)trimethoxysilane:

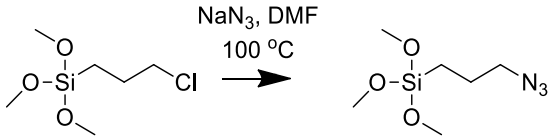

Anhydrous dimethylformamide (40 mL) was added to a flame-dried round bottom flask containing 3-chloropropyltrimethoxysilane (12 mL, 65.3 mmol, 1x) and sodium azide (6.38 g, 98.1 mmol, 1.5x) under argon. The reaction was stirred overnight at 100 ºC, upon which it was cooled to room temperature and diluted with 1:1 diethyl ether:water (150 mL). The organic layer was washed with water (3x) and brine (1x), dried over $MgSO_4$, and concentrated to yield a clear oil (12.741 g, 62.1 mmol, 95%). ^{1}H NMR (500 MHz, $CDCl_3$) δ 3.57 (s, 9H), 3.26 (t, J = 6.9 Hz, 2H), 1.75 – 1.66 (m, 2H), 0.73 – 0.66 (m, 2H); ^{13}C NMR (126 MHz, $CDCl_3$) δ 53.86, 50.72, 22.58, 6.46; HRMS (FAB+): calculated for $C_6H_{16}N_3O_3Si^+$ [M + ^{1}H]$^+$, 206.0961; found 206.0978. (Δ = +8.3 ppm). These spectral data matched those reported previously.[4]

Treatment of glass slides:

Plain glass micro slides (Corning) were cleaned with piranha solution (50% sulfuric acid, 35% dH_2O, 15% H_2O_2) for 30 min at room temperature. The slides were rinsed with water, acetone (3x) and then dried. The slides were incubated for 90 min in a toluene solution containing (3-azidopropyl)trimethoxysilane (70 mM) and n-butylamine (70 mM). The slides were subsequently rinsed with toluene, wiped dry with a Kimwipe, and baked overnight at 80 ºC. Functionalized slides were stable when stored at room temperature under ambient conditions for several weeks.

This silanization procedure was derived from the work by Walba, *et al*.[5]

DOI: 10.1038/NMAT4219

Method S4 Synthesis of heterobifunctional photocaged alkoxyamine/azide linker (N_3-TEG-ONH-NPPOC)

Synthesis of 2-(2-(2-(2-azidoethoxy)ethoxy)ethoxy)ethanol:

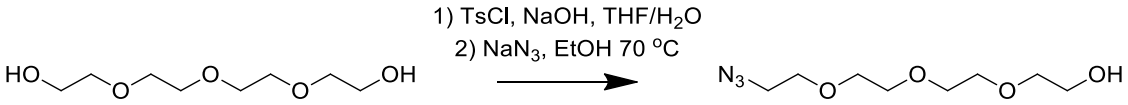

A 250-mL round bottom flask equipped with an oval-shaped magnetic stir bar was charged with tetraethylene glycol (50.9 g, 262 mmol, 10x) in tetrahydrofuran (10 mL). An aqueous solution (10 mL) containing sodium hydroxide (1.68 g, 42 mmol, 1.6x) was added to the flask, and p-toluenesulfonyl chloride (5 g, 26.2 mmol, 1x) dissolved in tetrahydrofuran (30 mL) was added dropwise to the mixture at 0 ºC and stirred while maintaining this temperature for 3 hr. The reaction was diluted with ice-cold water (150 mL) and extracted into dichloromethane (3 x 100 mL). The combined organic layers were washed with water (2 x 300 mL), dried over $MgSO_4$, filtered, and concentrated to yield a clear oil (9.2 g, 26.2 mmol, quantitative yield). Sodium azide (4.3 g, 65.5 mmol, 2.5x) was added to the tosylate intermediate, and the mixture was dissolved in absolute ethanol (200 mL). The reaction was stirred under reflux overnight, cooled to room temperature, and then diluted with water (150 mL). The mixture was concentrated by rotary evaporation to approximately 150 mL, and the product was extracted into ethyl acetate (3 x 150 mL), dried with $MgSO_4$, filtered, and concentrated to yield a faint yellow liquid (5.1 g, 23.3, 89% yield over two steps). ^{1}H NMR (500 MHz, $CDCl_3$) δ 3.72 – 3.69 (m, 2H), 3.67 – 3.64 (m, 10H), 3.61 – 3.58 (m, 2H), 3.38 (t, J = 5.0 Hz, 2H), 2.54 (s, 1H); ^{13}C NMR (126 MHz, $CDCl_3$) δ 72.47, 70.69, 70.65, 70.58, 70.34, 70.04, 61.73, 50.65; HRMS (EI+): calculated for $C_8H_{18}N_3O_4^+$ [M + ^{1}H]$^+$, 220.1297; found 220.1306 (Δ = +4.1 ppm).

Synthesis of 2-(2-(2-(2-(2-azidoethoxy)ethoxy)ethoxy)ethoxy)isoindoline-1,3-dione:

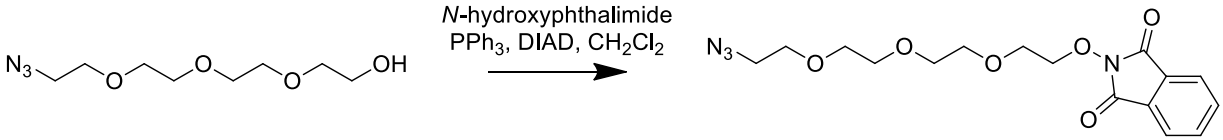

2-(2-(2-(2-azidoethoxy)ethoxy)ethoxy)ethanol (5.03 g, 23 mmol, 1x), triphenylphosphine (7.25 g, 27.6 mmol, 1.2x), *N*-hydroxyphthalimide (4.70 g, 28.8 mmol, 1.25x), and a magnetic stir bar were added to a flame-dried round bottom flask, purged with argon, dissolved in anhydrous dichloromethane (350 mL), and brought to 0 ºC. Diisopropyl azodicarboxylate (5.31 mL, 5.45 g, 27.0 mmol, 1.17x) was added dropwise, and the mixture was stirred overnight (0 ºC → RT). The crude reaction mixture was concentrated under reduced pressure and purified by flash chromatography (1:1 hexanes/EtOAc) to yield a pale yellow liquid (7.13 g, 19.6 mmol) in good yield (85%). ^{1}H NMR (500 MHz, $CDCl_3$) δ 7.82 (dd, J = 5.4, 3.1 Hz, 2H), 7.73 (dd, J = 5.5, 3.1 Hz, 2H), 4.38 – 4.34 (m, 2H), 3.87 – 3.83 (m, 2H), 3.67 – 3.62 (m, 4H), 3.62 – 3.56 (m, 6H), 3.36 (t, J = 5.6 Hz, 2H); ^{13}C NMR (126 MHz, $CDCl_3$) δ 163.42, 134.44, 128.96, 123.47, 77.21, 70.78, 70.60, 70.59, 70.56, 70.00, 69.28, 50.67; HRMS (EI+): calculated for $C_{16}H_{21}N_4O_6^+$ [M + ^{1}H]$^+$, 365.1461; found 365.1457 (Δ = -1.1 ppm).

Synthesis of O-(2-(2-(2-(2-azidoethoxy)ethoxy)ethoxy)ethyl)hydroxylamine (N_3-TEG-ONH_2):

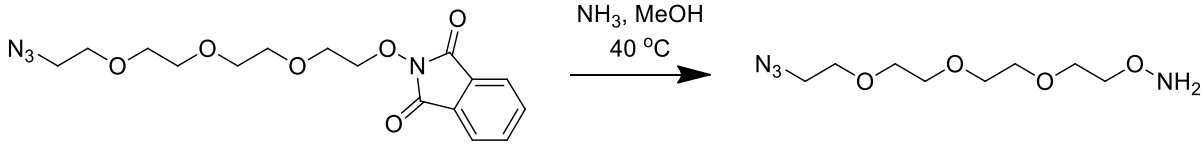

2-(2-(2-(2-(2-azidoethoxy)ethoxy)ethoxy)ethoxy)isoindoline-1,3-dione (2.60 g, 7.14 mmol) was purged with nitrogen and then treated overnight at 40 ºC with methanolic ammonia (7 N in MeOH, 300 mL). The reaction mixture was concentrated under reduced pressure, resuspended in dichloromethane (300 mL), filtered, and concentrated *in vacuo* once more. Purified product (N_3-TEG-ONH_2, 1.32 g, 5.64 mmol, 79%) was obtained as a clear liquid following semipreparative reversed-phase high-performance liquid chromatography (RP-HPLC, Thermo Scientific Dionex UltiMate 3000) using a 50 min linear gradient (5 – 100%) of acetonitrile and 0.1% trifluoroacetic acid and lyophilization. ^{1}H NMR (500 MHz, $CDCl_3$) δ 4.26 – 4.22 (m, 2H), 3.87 – 3.84 (m, 2H), 3.74 – 3.70 (m, 2H), 3.68 – 3.63 (m, 8H), 3.48 (t, J = 5.6, 2H); ^{13}C NMR (126 MHz, $CDCl_3$) δ 73.05, 70.69, 70.42, 70.27, 70.16, 69.73, 69.67, 50.89; HRMS (FAB+): calculated for $C_8H_{19}N_4O_4^+$ [M + ^{1}H]$^+$, 235.1406; found 235.1401 (Δ = -2.2 ppm). These spectral data matched those reported previously.[6]

Synthesis of 2-(2-nitrophenyl)propan-1-ol:

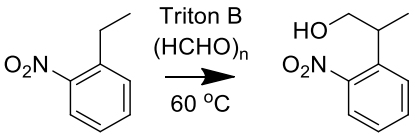

Paraformaldehyde (4.51 g, 150 mmol, 1.23x), 1-ethyl-2-nitrobenzene (16.4 mL, 18.48 g, 122 mmol, 1x), and benzyltrimethylammonium hydroxide (triton B, 50 mL of a 40 wt% solution in methanol, 20 g, 120 mmol, 1x) were charged into a round bottom flask and heated under reflux (60 ºC) overnight. The reaction mixture was concentrated, neutralized with 1 N HCl (200 mL), and extracted with ethyl acetate (3 x 200 mL). The combined organic layers were dried over $MgSO_4$, filtered, concentrated under reduced pressure, and the residue was purified by flash column chromatography on silica gel (4:1 to 2:1 hexanes/EtOAc) to afford a red oil (16.7 g, 92.1 mmol) in good yield (77%). ^{1}H NMR (500 MHz, $CDCl_3$) δ 7.75 (ddd, J = 8.2, 1.4, 0.4 Hz, 1H), 7.57 (tdd, J = 7.3, 1.4, 0.7 Hz, 1H), 7.49 (dd, J = 7.9, 1.4 Hz, 1H), 7.36 (ddd, J = 8.1, 7.3, 1.4 Hz, 1H), 3.85 – 3.72 (m, 2H), 3.57 – 3.45 (m, 1H), 1.65 (s, 1H), 1.33 (d, J = 6.9 Hz, 3H); ^{13}C NMR (126 MHz, $CDCl_3$) δ 138.08, 132.65, 128.19, 127.20 (2C), 124.10, 67.88, 36.37, 17.56; HRMS (FAB+): calculated for $C_9H_{12}NO_3^+$ [M + ^{1}H]$^+$, 182.0817; found 182.0861 (Δ = +24 ppm).

DOI: 10.1038/NMAT4219

Synthesis of 2,5-dioxopyrrolidin-1-yl (2-(2-nitrophenyl)propyl) carbonate (NPPOC-OSu):

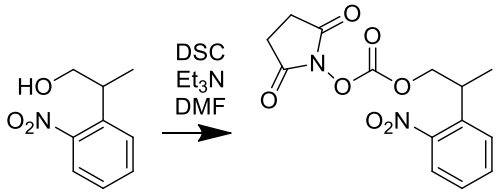

N,N'-Disuccinimidyl carbonate (10.13 g, 39.5 mmol, 1.5x) dissolved in anhydrous dimethylformamide (115 mL) was added to a round bottom flask containing 2-(2-nitrophenyl)propan-1-ol (4.78 g, 26.4 mmol, 1x). Triethylamine (20.2 mL, 14.67 g, 145 mmol, 5.5x) was added dropwise, and the reaction mixture was stirred overnight protected from light. The reaction mixture was concentrated under reduced pressure and purified on silica by flash column chromatography (4:1 to 1:1 hexanes/EtOAc) to yield a dark red oil (NPPOC-OSu, 6.24 g, 19.4 mmol) in good yield (73%). ^{1}H NMR (500 MHz, $CDCl_3$) δ 7.82 (dd, J = 8.2, 1.4 Hz, 1H), 7.64 – 7.59 (m, 1H), 7.50 (dd, J = 7.9, 1.4 Hz, 1H), 7.42 (ddd, J = 8.1, 7.4, 1.4 Hz, 1H), 4.59 – 4.45 (m, 2H), 3.80 (q, J = 6.5 Hz, 1H), 2.81 (s, 4H), 1.43 (d, J = 7.0 Hz, 3H); ^{13}C NMR (126 MHz, $CDCl_3$) δ 168.58, 151.56, 150.09, 135.96, 133.21, 128.67, 128.1, 124.71, 74.56, 33.50, 29.85, 25.56, 17.63; HRMS (EI+): calculated for $C_{17}H_{12}N_3O_4^+$ [M + ^{1}H]$^+$, 322.0828; found 322.0820 (Δ = -2.5 ppm). These spectral data matched those reported previously.[7]

Synthesis of 2-(2-nitrophenyl)propyl 2-(2-(2-(2-azidoethoxy)ethoxy)ethoxy)ethoxycarbamate (N_3-TEG-ONH-NPPOC)

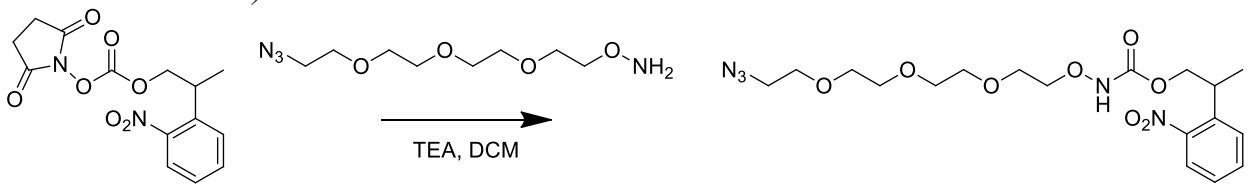

N_3-TEG-ONH_2 (90 mg, 0.38 mmol, 1x) and NPPOC-OSu (247.6 mg, 0.77 mmol, 2x) were purged with argon and then dissolved in anhydrous dichloromethane (10 mL). Triethylamine (214 µL, 156 mg, 1.54 mmol, 4x) was added, and the reaction mixture was stirred overnight protected from light. Solvent was removed by rotary evaporation, and the residue was purified by semipreparative reversed-phase high-performance liquid chromatography (RP-HPLC, Thermo Scientific Dionex UltiMate 3000) using a 50 min linear gradient (5 – 100%) of acetonitrile and 0.1% trifluoroacetic acid. Upon lyophilization, the clear liquid product (N_3-TEG-ONH-NPPOC, 138 mg, 0.31 mmol) was obtained in good yield (82%). ^{1}H NMR (500 MHz, $CDCl_3$) δ 7.89 (s, 1H), 7.75 (dd, J = 8.1, 1.3 Hz, 1H), 7.60 – 7.54 (m, 1H), 7.50 – 7.45 (m, 1H), 7.40 – 7.34 (m, 1H), 4.35 – 4.23 (m, 2H), 3.99 – 3.91 (m, 2H), 3.70 – 3.68 (m, 2H), 3.67 – 3.63 (m, 11H), 3.38 (t, J = 5.0 Hz, 2H), 1.36 (d, J = 7.0 Hz, 3H); ^{13}C NMR (126 MHz, $CDCl_3$) δ 157.02, 150.60, 137.14, 132.81, 128.22, 127.60, 124.23, 75.50, 70.76, 70.69, 70.66, 70.63, 70.11, 69.39, 69.31, 50.76, 33.39, 17.78; HRMS (FAB+): calculated for $C_{18}H_{28}N_5O_8^+$ [M + ^{1}H]$^+$, 442.1938; found 442.1921 (Δ = -3.8 ppm).

Method S5 Synthesis of amine-reactive aldehyde linker for protein labeling (NHS-CHO)

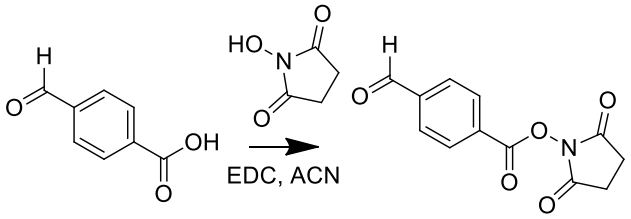

NHS-CHO was synthesized *via* a known synthetic route.[8] 4-formylbenzoic acid (2 g, 13.3 mmol, 1x), *N*-Hydroxysuccinimide (1.69 g, 14.6 mmol, 1.1x), and *N*-(3-Dimethylaminopropyl)-*N*′-ethylcarbodiimide hydrochloride (EDC·HCl, 2.81 g, 14.6 mmol, 1.1x) were dissolved in anhydrous acetonitrile (50 mL) under argon. After stirring overnight at room temperature, the solvent was removed under reduced pressure, and the residue was resuspended in dichloromethane (100 mL). The organic layers were washed with water (3x), dried over $MgSO_4$, filtered, and concentrated to yield quantitatively the pure product (2,5-dioxopyrrolidin-1-yl 4-formylbenzoate, NHS-CHO, 3.29 g, 13.3 mmol) as a white solid. ^{1}H NMR (500 MHz, $CDCl_3$) δ 10.13 (s, 1H), 8.32 – 8.26 (m, 2H), 8.05 – 7.99 (m, 2H), 2.93 (s, 4H); ^{13}C NMR (126 MHz, $CDCl_3$) δ 191.30, 169.08, 161.17, 140.45, 131.30, 130.08, 129.85, 25.80; HRMS (FAB+): calculated for $C_{12}H_{10}NO_5^+$ $[M + {}^{1}H]^+$, 248.0559; found 248.0569 (Δ = +4.1 ppm).

DOI: 10.1038/NMAT4219

Method S6 Synthesis of amine-reactive aldehyde photocleavable linker for protein labeling (NHS-*o*NB-CHO)

Synthesis of 4-(4-(1-((4-(4-formylbenzamido)butanoyl)oxy)ethyl)-2-methoxy-5-nitrophenoxy) butanoic acid (HOOC-oNB-CHO):

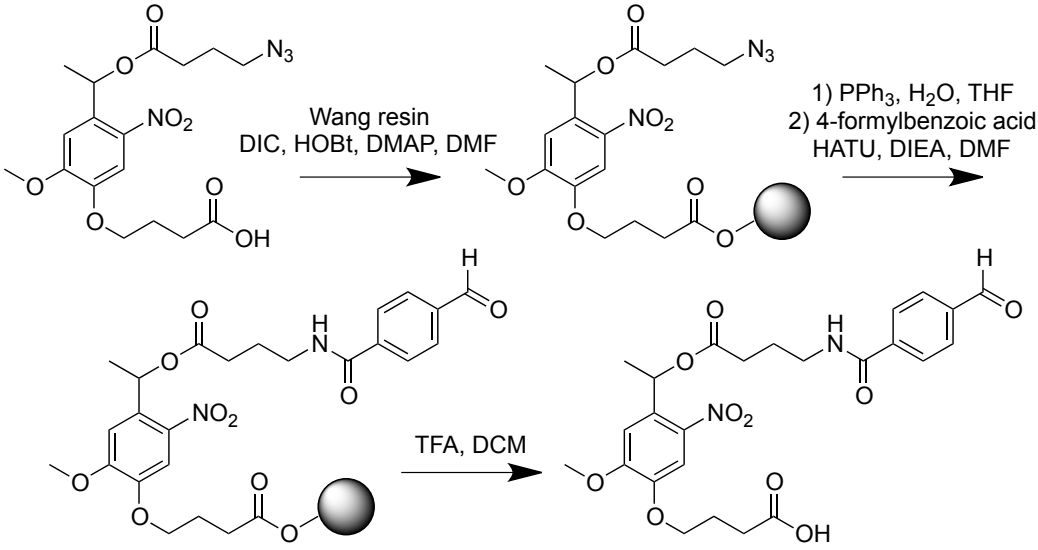

4-(4-(1-((4-azidobutanoyl)oxy)ethyl)-2-methoxy-5-nitrophenoxy)butanoic acid (369 mg, 0.9 mmol, 2x) was synthesized following a known synthetic route[3] and then dissolved with hydroxybenzotriazole (HOBt, 122 mg, 0.9 mmol, 2x) in minimal dimethylformamide. *N,N'*-Diisopropylcarbodiimide (DIC, 116 mg, 0.9 mmol, 2x) and 4-dimethylaminopyridine (DMAP, 5.5 mg, 0.045 mmol, 0.1x) were combined in a separate vial and dissolved in minimal dimethylformamide. The combined solutions were added to Wang resin (0.45 mmol OH, 0.5 g, 0.9 mmol OH/g resin, EMD Millipore) preswollen in dichloromethane/dimethylformamide (9:1, 10 mL) and mixed for 3 hr protected from light. Resin was treated with 5 wt% triphenylphosphine in tetrahydrofuran/water (10:1) for 12 hours to reduce the terminal azide. 4-formylbenzoic acid (270 mg, 1.8 mmol, 4x), preactivated with 1-[bis(dimethylamino)methylene]-1H-1,2,3-triazolo[4,5-b]pyridinium 3-oxid hexafluorophosphate (HATU, 676 mg, 1.78 mmol, 3.95x) and *N,N*-diisopropylethylamine (DIEA, 627 µL, 465 mg, 3.6 mmol, 8x) in dimethylformamide, was coupled to the primary amine *via* standard peptide chemistry. Resin was treated with trifluoroacetic acid (20%) in dichloromethane for 15 min, upon which the supernatant was concentrated under reduced pressure and purified by reversed-phase high-performance liquid chromatography (RP-HPLC, Thermo Scientific Dionex UltiMate 3000) using a 55 min linear gradient (25 – 100%) of acetonitrile and 0.1% trifluoroacetic acid. The product was lyophilized to give a yellow solid (HOOC-*o*NB-CHO, 102 mg, 0.20 mmol) in moderate yield (44% over four steps). ^{1}H NMR (500 MHz, DMSO-d6) δ 12.16 (br s, 1H), 10.07 (s, 1H), 8.67 (t, J = 5.6 Hz, 1H), 7.98 (s, 4H), 7.55 (s, 1H), 7.09 (s, 1H), 6.20 (q, J = 6.4 Hz, 1H), 4.06 (t, J = 6.5 Hz, 2H), 3.91 (s, 3H), 3.28 (td, J = 6.9, 5.6 Hz, 2H), 2.46 – 2.41 (m, 2H), 2.38 (t, J = 7.3 Hz, 2H), 1.99 – 1.91 (m, 2H), 1.83 – 1.73 (m, 2H), 1.56 (d, J = 6.5 Hz, 3H); ^{13}C NMR (126 MHz, DMSO-d6) δ 192.91, 173.98, 171.96, 165.42, 153.54, 146.83, 139.55, 139.48, 137.68, 132.03, 129.35, 127.85, 108.62, 108.38, 67.91, 67.33, 56.21, 38.65, 31.13, 29.93, 24.28, 23.98, 21.40. HRMS (FAB+): calculated for $C_{25}H_{28}NaN_2O_{10}^+$ [M + ^{11}Na]$^+$, 539.1641; found 539.1636 (Δ = -0.9 ppm).

Synthesis of 2,5-dioxopyrrolidin-1-yl 4-(4-(1-((4-(4-formylbenzamido)butanoyl)oxy)ethyl)-2-methoxy-5-nitrophenoxy)butanoate (NHS-oNB-CHO)

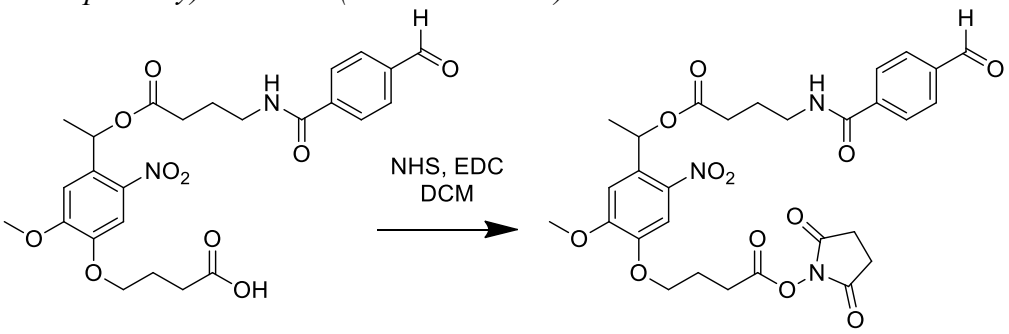

HOOC-*o*NB-CHO (70 mg, 0.14 mmol, 1x), *N*-hydroxysuccinimide (17 mg, 0.15 mmol, 1.1x), and *N*-(3-dimethylaminopropyl)-*N*′-ethylcarbodiimide hydrochloride (EDC·HCl, 29 mg, 0.15 mmol, 1.1x) were combined in a scintillation vial containing a magnetic stir bar, dissolved in anhydrous acetonitrile (3 mL) and stirred overnight protected from light. The reaction mixture was concentrated *in vacuo*, washed with water (3x), dried over $MgSO_4$, filtered, and concentrated once more to yield a pale yellow oil (NHS-*o*NB-CHO, 77 mg, 0.13 mmol) in good yield (93%). ^{1}H NMR (500 MHz, DMSO-d6) δ 10.08 (s, 1H), 8.67 (t, J = 5.6 Hz, 1H), 7.99 (s, 4H), 7.55 (s, 1H), 7.10 (s, 1H), 6.21 (q, J = 6.4 Hz, 1H), 4.16 (t, J = 6.5 Hz, 2H), 3.92 (s, 3H), 3.28 (td, J = 6.9, 5.6 Hz, 2H), 2.85 (t, J = 7.3 Hz, 2H), 2.83 (s, 4H), 2.47 – 2.41 (m, 2H), 2.14 – 2.06 (m, 2H), 1.84 – 1.74 (m, 2H), 1.57 (d, J = 6.5 Hz, 3H); ^{13}C NMR (126 MHz, DMSO-d6) δ 192.92, 171.97, 170.21, 168.64, 165.45, 153.56, 146.85, 139.57, 139.51, 137.68, 132.04, 129.38, 127.86, 108.64, 108.39, 67.94, 67.32, 56.20, 38.67, 31.15, 26.94, 25.47, 24.28, 23.99, 21.44; HRMS (EI+): calculated for $C_{29}H_{32}N_3O_{12}^+$ [M + ^{1}H]$^+$, 614.1986; found 614.1995 (Δ = +1.5 ppm).

DOI: 10.1038/NMAT4219

Method S7 Introduction of aldehydes onto proteins upon reaction with NHS-CHO or NHS-*o*NB-CHO

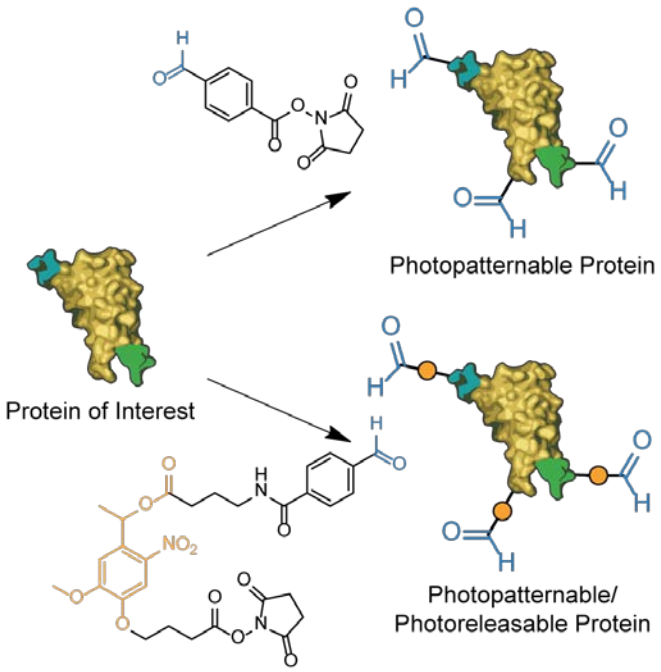

Synthesis of aldehyde-functionalized bovine serum albumin (BSA-CHO and BSA_{488}-CHO)
Bovine serum albumin (10 mg, 0.15 µmol, 9 µmol primary amines) was dissolved in aqueous sodium bicarbonate (0.1 M, pH = 8.3). NHS-CHO (0.38 mg, 1.55 µmol, 38.4 µL of a 10 mg mL^{-1} stock solution in anhydrous dimethylformamide) was added to the protein mixture. Optionally, AlexaFluor 488 carboxylic acid, succinimidyl ester (0.5 mg, 0.77 µmol, 50 µL of a 10 mg mL^{-1} stock solution in anhydrous dimethylformamide, Invitrogen) was also included. The reactions were mixed on a shaker wheel for 2 hrs at 25 ºC prior to dialysis (molecular weight cutoff ~ 2 kDa, SpectraPor) and lyophilization. The aldehyde-functionalized product and its fluorescent counterpart (denoted BSA-CHO and BSA_{488}-CHO, respectively) were used with no additional purification.

Synthesis of photoreleasable aldehyde-functionalized bovine serum albumin (BSA-oNB-CHO, BSA_{488}-oNB-CHO, and BSA_{594}-oNB-CHO)
Bovine serum albumin (10 mg, 0.15 µmol, 9 µmol primary amines) was dissolved in aqueous sodium bicarbonate (0.1 M, pH = 8.3). NHS-*o*NB-CHO (0.80 mg, 1.55 µmol, 80.3 µL of a 10 mg mL^{-1} stock solution in anhydrous dimethylformamide) was added to the protein mixture. Optionally, AlexaFluor 488 carboxylic acid, succinimidyl ester (0.5 mg, 0.77 µmol, 50 µL of a 10 mg mL^{-1} stock solution in anhydrous dimethylformamide, Invitrogen) or AlexaFluor 594 carboxylic acid, succinimidyl ester (0.5 mg, 0.61 µmol, 50 µL of a 10 mg mL^{-1} stock solution in anhydrous dimethylformamide, Invitrogen) was also included. The reactions were mixed on a shaker wheel for 2 hrs at 25 ºC prior to dialysis (molecular weight cutoff ~ 2 kDa, SpectraPor) and lyophilization. The aldehyde-functionalized product and its green and red fluorescent counterparts (denoted BSA-*o*NB-CHO, BSA_{488}-*o*NB-CHO, and BSA_{594}-*o*NB-CHO, respectively) were used with no additional purification.

Synthesis of aldehyde-functionalized vitronectin variants (VTN_{488}-oNB-CHO, VTN_{488}-CHO, and VTN-oNB-CHO).
VTN_{488}-*o*NB-CHO, VTN_{488}-CHO, and VTN-*o*NB-CHO were synthesized from vitronectin (Invitrogen) following the procedures previously described for BSA_{488}-*o*NB-CHO, BSA_{488}-CHO, and BSA-*o*NB-CHO, respectively.

Synthesis of additional photoreleasable aldehyde-functionalized proteins
Collagenase (Sigma), mouse anti-6xHis primary antibody (Invitrogen), and Delta (a generous gift from the Murry and Bernstein laboratories at the University of Washington) were functionalized upon treatment of NHS-*o*NB-CHO following the procedures described previously for BSA-*o*NB-CHO.

DOI: 10.1038/NMAT4219

Method S8 Synthesis of self-quenched collagenase-sensitive detection peptide (FAM-RGLGPAGRK(FAM)-NH_2)

The base peptide H-RGLGPAGRK(dde)-NH_2 was synthesized on rink amide resin (NovaBioChem) *via* standard microwave-assisted Fmoc solid phase methodology and HATU activation (CEM Liberty 1). The 1-(4,4-dimethyl-2,6-dioxacyclohexylidene)ethyl (dde) group was removed with 2% hydrazine monohydrate in dimethylformamide (3 x 10 min), and 5(6)-carboxyfluorescein (FAM, Fisher) was coupled simultaneously to the N-terminal amine and the ε-amino group of the C-terminal lysine with HATU (Chem-Impex). Resin was treated with trifluoroacetic acid/triisopropylsilane/water (95:2.5:2.5) for 2 hr, and the crude peptide was precipitated in and washed (2x) with ice-cold diethyl ether. The crude peptide was purified using semi-preparative reversed-phase high-performance liquid chromatography (RP-HPLC) using a 60 min linear gradient (5–50% of acetonitrile and 0.1% trifluoroacetic acid) and lyophilized to give the product (FAM-RGLGPAGRK(FAM)-NH_2) as a fluffy, orange solid. Peptide purity was confirmed with analytical RP-HPLC and matrix-assisted laser desorption-ionization time-of-flight mass spectrometry using α-cyano-4-hydroxycinnamic acid matrix: MALDI-TOF: calculated for $C_{80}H_{92}N_{17}O_{21}^+$ $[M + {}^1H]^+$, 1626.7; found 1627.3.

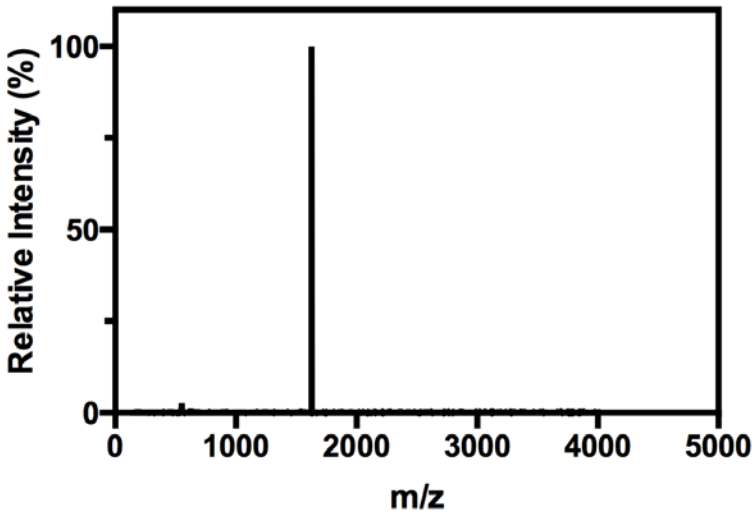

Figure S1 ***In situ*** **rheometry of gel formation and effects of hydrogel formulation on final moduli**

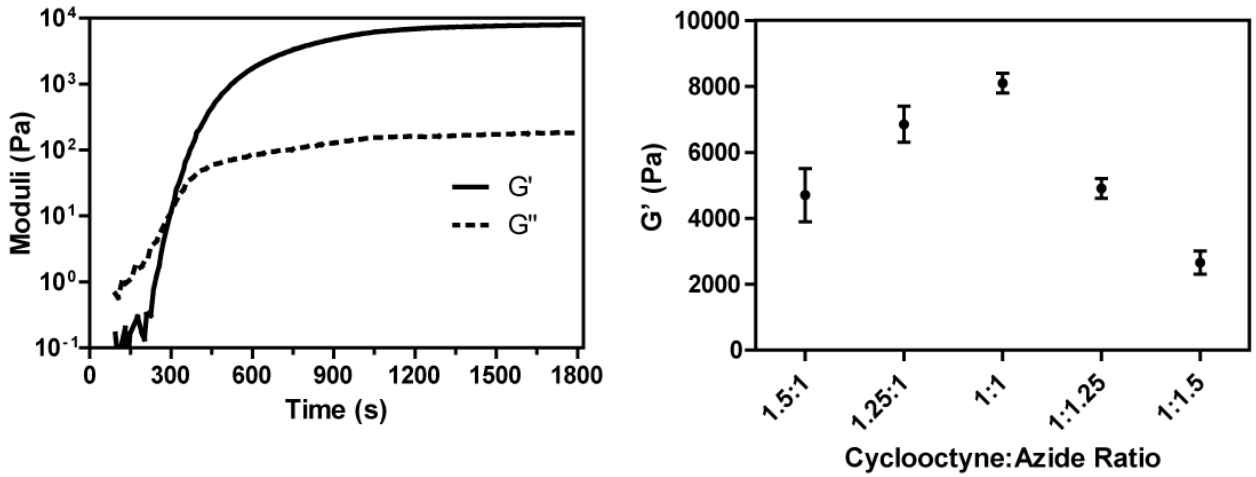

Dynamic frequency-, time-, and strain-sweep rheological experiments were performed on a TA Instruments ARES rheometer with parallel-plate geometry (25 mm diameter) at 25 °C. Initial network formation of a 10 wt% solution was monitored by observing G' and G'' at a constant frequency of 100 rad s^{-1} as a function of time. Gel properties were monitored *via* frequency-sweep measurements at fixed strain amplitude (10%) to measure the hydrogel storage (G') and loss (G'') moduli. The crossover point of stoichiometrically-balanced gels (cyclooctyne:azide = 1) was found to be at 315 ± 10 sec, and the final modulus was determined to be 8100 ± 300 Pa (left). When hydrogels (10 wt%) were formed off-stoichiometrically, a decrease in overall network stiffness was observed corresponding to the decreased crosslinking density (right).

DOI: 10.1038/NMAT4219

Figure S2 NMR kinetic studies of N_3-TEG-ONH-NPPOC photouncaging

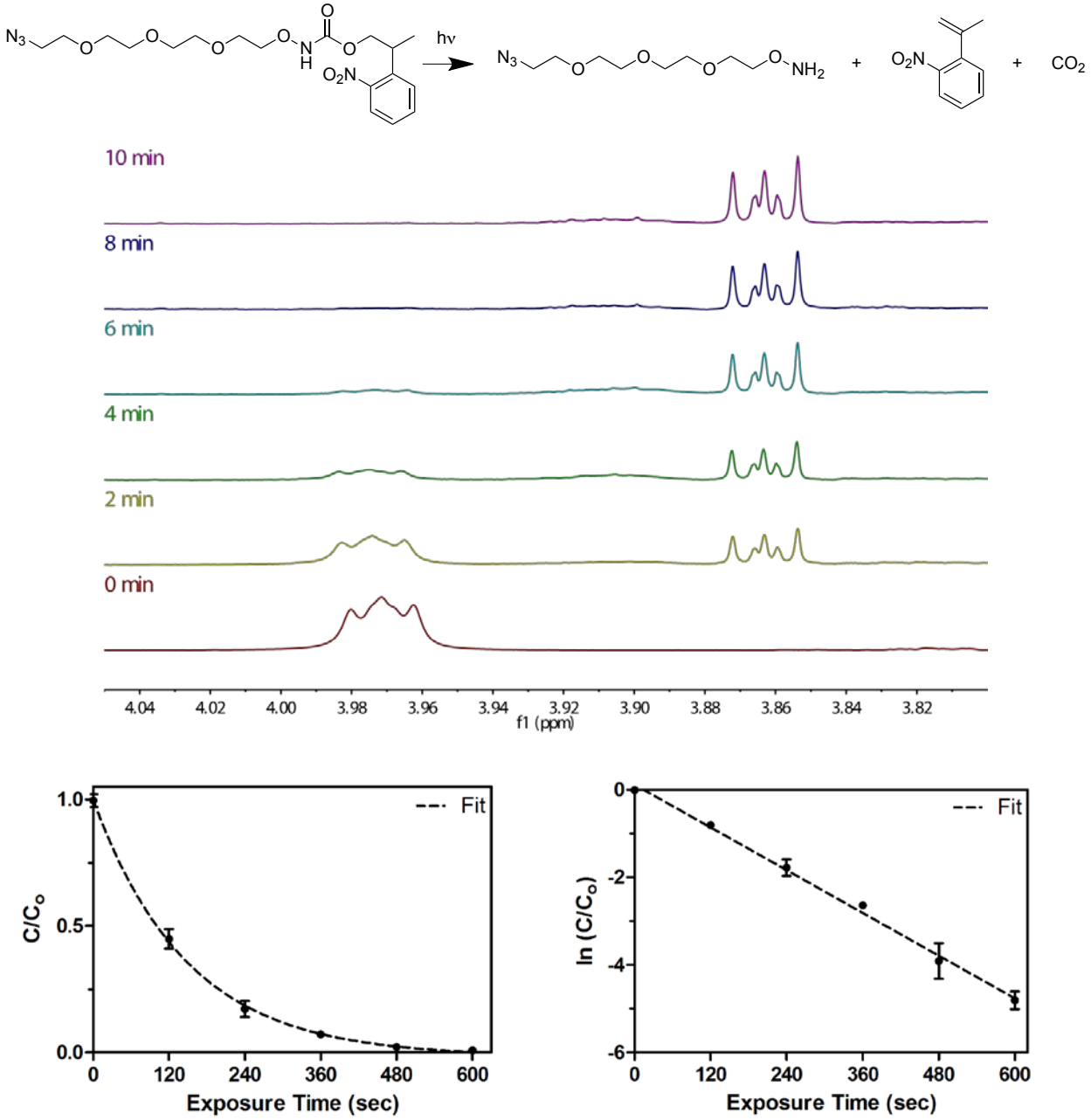

Aqueous N_3-TEG-ONH-NPPOC (1 mM) was injected into a glass sample chamber measuring 4 cm x 4 cm x 2 mm. Samples were exposed to collimated light (λ = 365 nm, 10 mW cm^{-2}) in batches (4 x 3 mL) for various amounts of time (0 – 10 min) to induce NPPOC photodissociation. Samples from each exposure condition were combined, lyophilized, and resuspended in $CDCl_3$ (600 µL) prior to ^1H NMR analysis. The fraction of uncaging was calculated by comparing the NMR signal intensities corresponding to the α-protons of the aminooxy carbamate starting material (δ = 3.97, 2H) and the α-hydrogens of the uncaged alkoxyamine (δ = 3.86, 2H).

The NPPOC photodeprotection process follows first-order reaction kinetics:

$$\frac{C}{C_0} = e^{-k \cdot t}$$

where C is the concentration of intact NPPOC cage at any time t, C_0 is the initial concentration of the N_3-TEG-ONH-NPPOC (1 mM), and k is the kinetic constant of photocleavage. As >95% of the 365 nm light is transmitted throughout our 2 mm thick sample, the effects of attenuation have been ignored in this analysis and light intensity is assumed to be uniform throughout the solution. From the equation above, it follows that:

$$\ln \frac{C}{C_0} = -k \cdot t$$

Plotting our data (bottom left) in this form (bottom right) gives us a linear plot with a slope:

$$k = 0.0067 \pm 0.0005 \frac{1}{\text{sec}}$$

for $\lambda = 365$ nm at 10 mW cm^{-2}.

The quantum yield (ϕ) for this system is given by[9]:

$$\varphi = \frac{N_A h \nu k}{\varepsilon I}$$

where N_A is Avogadro's number, h is the Planck constant, ν is the frequency of the associated electromagnetic wave, ε is the molar absorptivity of the sample (285 M^{-1} cm^{-1} for N_3-TEG-ONH-NPPOC at λ = 365 nm, Supplementary Fig. S3); and I is the intensity of light. Thus, all variables in the equation for ϕ are known:

$$\varphi = 0.73$$

Using this quantum yield, the kinetic constant of NPPOC photouncaging is calculated readily for any light intensity as:

$$k = \frac{\varphi \varepsilon I}{N_A h \nu}$$

DOI: 10.1038/NMAT4219

Figure S3 Colorimetric shift from NPPOC photouncaging

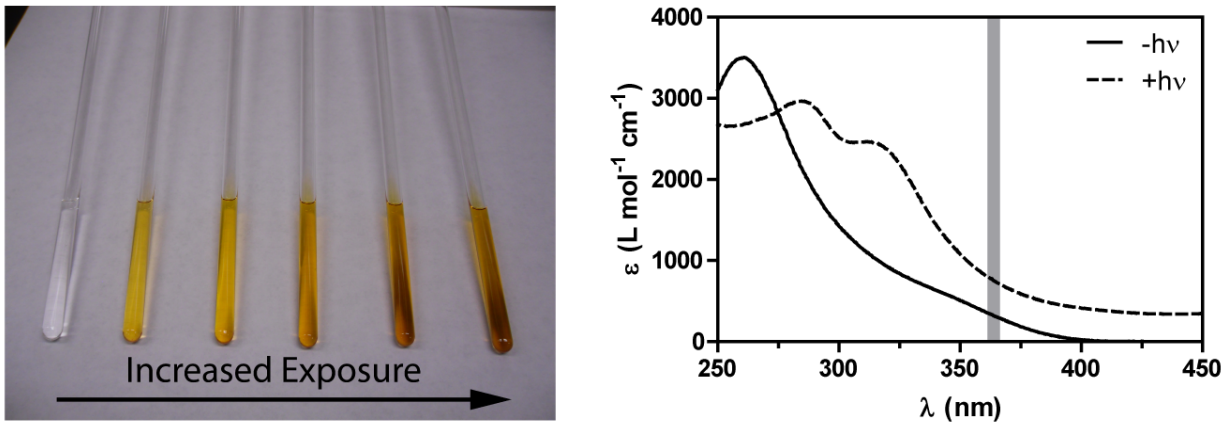

Light-exposed samples from Figure S2 (0, 2, 4, 6, 8, 10 min exposure from left to right) were visualized with digital photography (left) and UV-Vis spectrometry (right, data from 0 and 10 minute exposures).

Figure S4 Determining the extent of protein functionalization by fluorescence labeling

Fluorescence labeling of proteins:

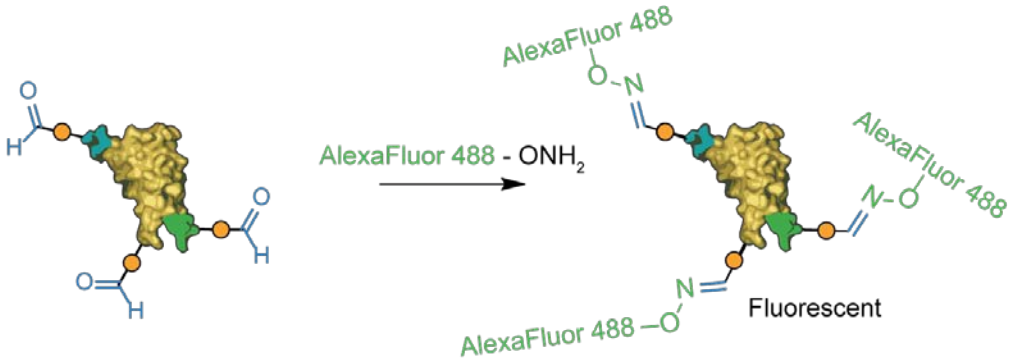

BSA-*o*NB-CHO (5 mg, 0.075 μmol, 1x) was dissolved in phosphate-buffered saline (pH = 6.5, 250 μL). AlexaFluor 488 C5-aminooxyacetamide, bis(triethylammonium) salt (0.67 mg, 0.75 μmol, 10x, Invitrogen) dissolved in dimethyl sulfoxide (67 uL) was added to the protein and reacted overnight protected from light. The reaction mixture was diluted with water and dialyzed (molecular weight cutoff ~ 2 kDa, SpectraPor) for 2 days and lyophilized to yield a yellow powder (denoted BSA-*o*NB-AF_{488}).

Quantification of fluorescence labeling:

Because ligation of the aminooxy-dye and the protein occurs exclusively through the aldehyde functionality, the extent of protein *o*NB-CHO functionalization can be estimated by determining the number of fluorescent moieties per protein. BSA-*o*NB-AF_{488} was dissolved in dH_2O at a known concentration ($c_{protein}$ = 0.15 mg mL^{-1} = 2.26 μM) and the Beer-Lambert law was used to estimate the number of fluorophores per protein (c_{dye}):

$$c_{dye} = \frac{A_{dye}}{\varepsilon_{dye} b}$$

where A_{dye} is the absorbance of the fluorophore-functionalized protein at λ = 495 nm, ε_{dye} is the molar absorptivity of AlexaFluor 488 at λ = 495 nm (ε_{dye} = 71,000 cm^{-1} M^{-1})[10], and b is the path length of the light (b = 1 cm). A_{dye} was quantified with UV-Vis spectroscopy to be 0.36 ± 0.01, we have:

$$c_{dye} = \frac{0.36}{\left(71000 \ \frac{1}{\text{cm M}}\right)(1 \text{ cm})} = 5.1 \text{ x } 10^{-6} \text{ M} = 5.1 \text{ μM}$$

The number of fluorophores per protein was determined as:

$$\text{Dye molecules per protein} = \frac{c_{dye}}{c_{protein}} = 2.25$$

DOI: 10.1038/NMAT4219

Based on this analysis, at least 2.25 of the 60 primary amines on BSA (59 lysine residues + N-terminus) were modified *via* NHS chemistry with aldehyde functionalities, corresponding to 3.8% modification.

Figure S5 Quantification of immobilized protein concentration

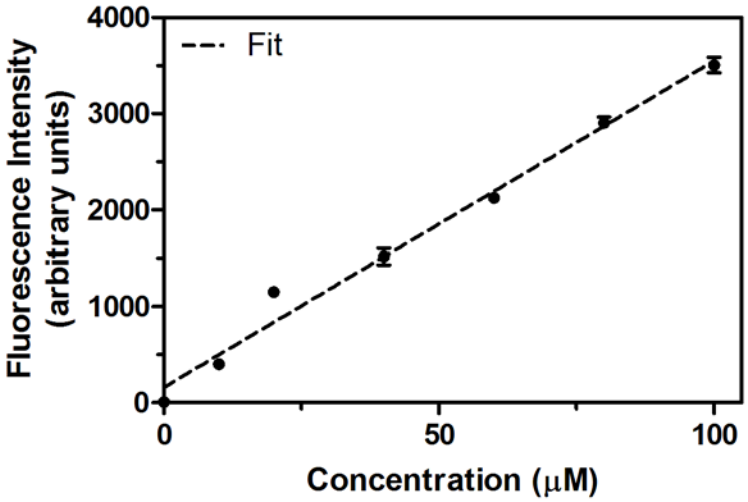

The level of BSA_{488}-*o*NB-CHO incorporation was quantified by comparing the patterned fluorescence ($\lambda_{excitation}$ = 488 nm) against known concentrations of the free protein in solution. The linear relationship between protein concentration and fluorescence was used to calculate the concentration of immobilized proteins within the SPAAC-based networks.

DOI: 10.1038/NMAT4219

Figure S6 Dose response for photo-mediated immobilization of proteins

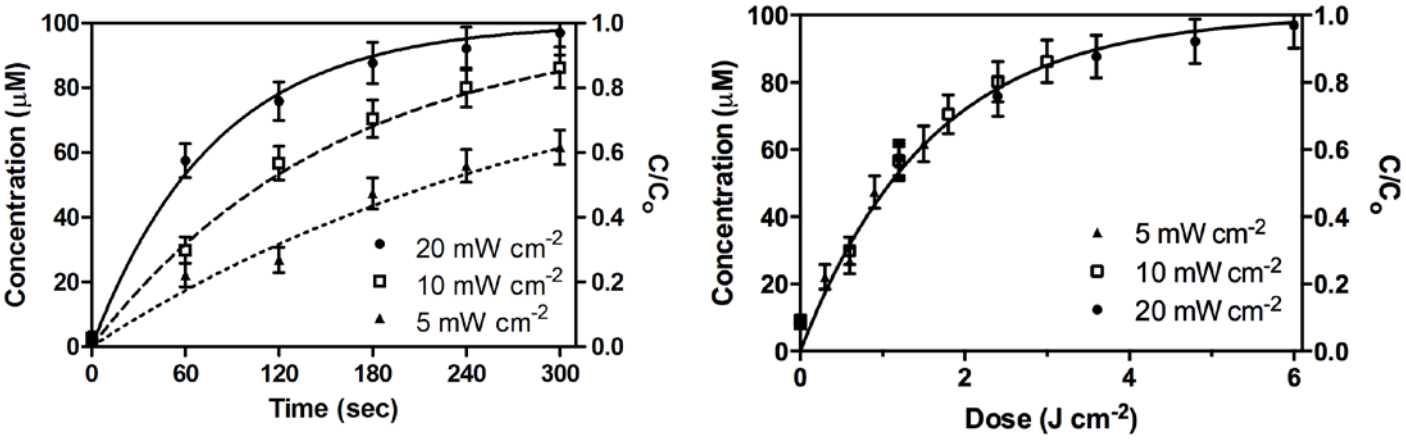

Dose represents the total amount of energy delivered to the system and was calculated as the product of exposure time and light intensity. Connected lines represent predicted concentration based on NPPOC cleavage photokinetics (Supplementary Fig. S2).

Figure S7 Schematic of protein gradient generation

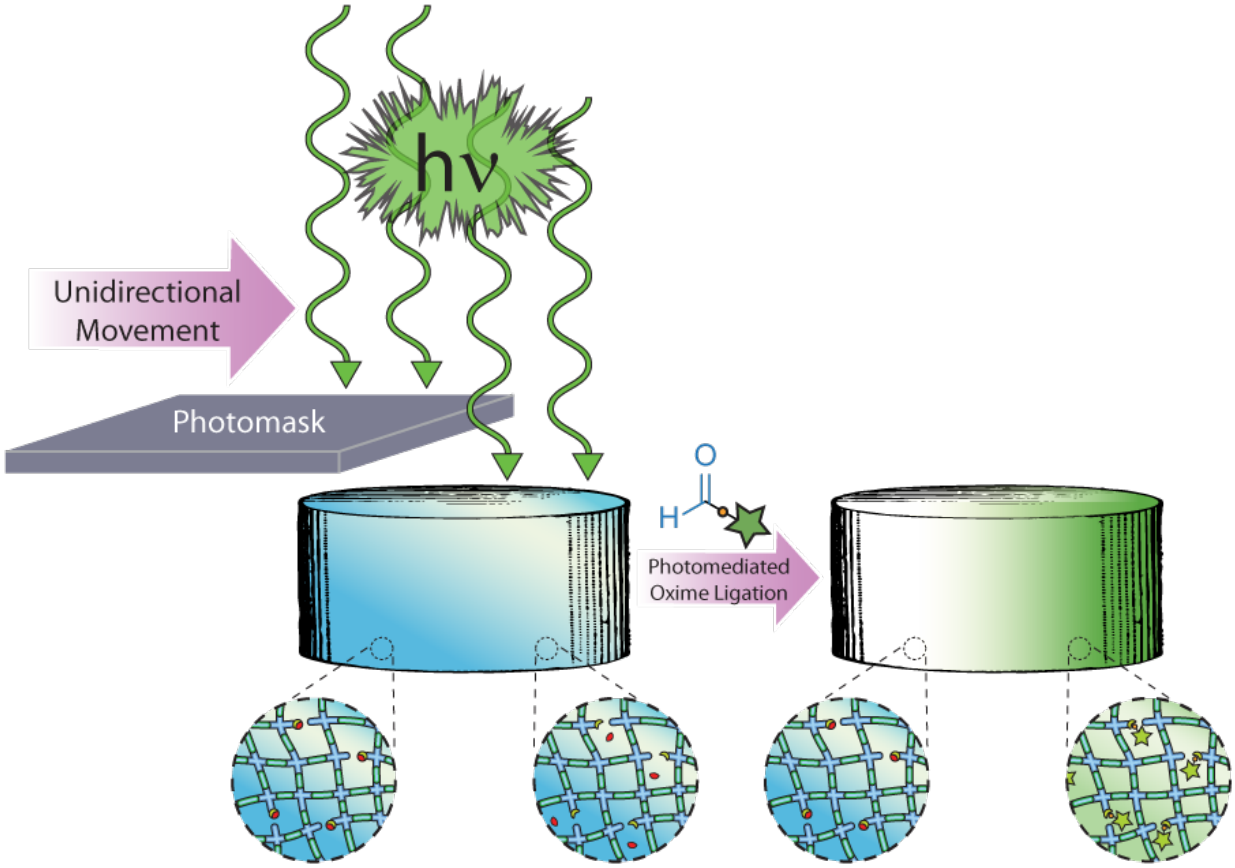

A solid photomask attached to a programmable linear motion stage (Harvard Apparatus PHD 2000 Syringe Pump) was used to define gradients of light exposure[11] across hydrogel surfaces. Gels were exposed to collimated UV light (λ = 365 nm, 10 mW cm^{-2}) while the sample was shielded with an opaque photomask moving at different rates (0.6, 1.2, and 2.4 mm min^{-1}). As the mask moves unidirectionally above the material, light is blocked from reaching the underlying sample, allowing for well-defined gradients of exposure. This platform was used to generate biochemical gradients through both the photomediated-immobilization and subsequent photorelease of *o*NB-CHO-functionalized proteins.

DOI: 10.1038/NMAT4219

Figure S8 Quantification of 3D protein patterning *via* photomediated oxime ligation

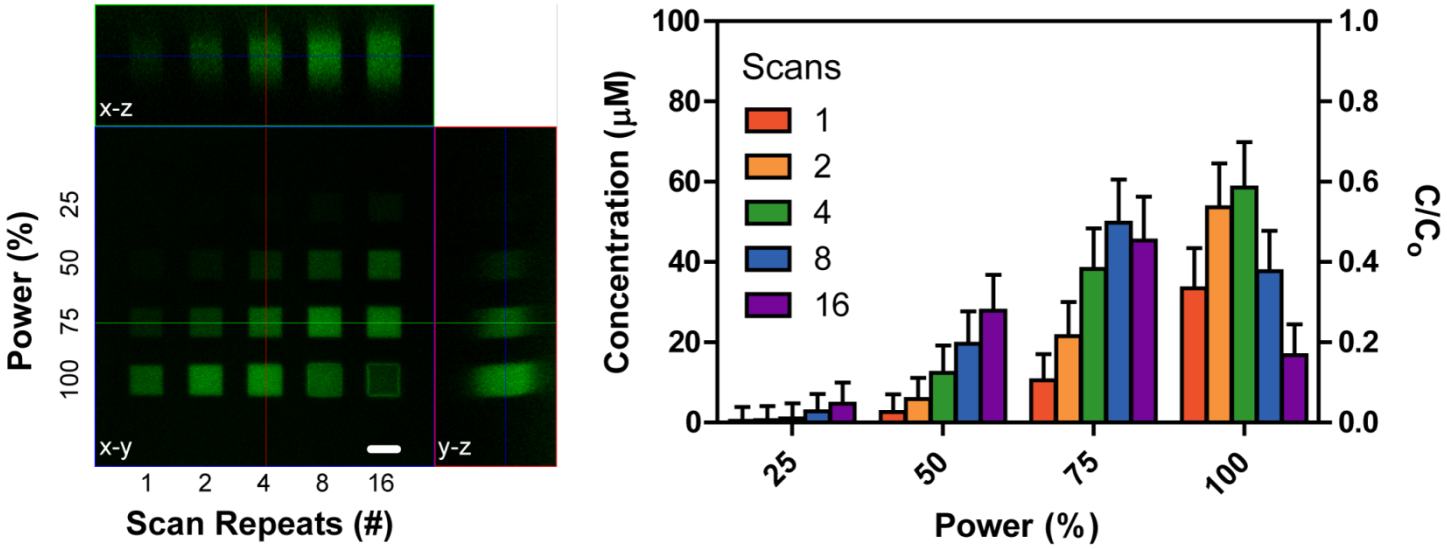

Multiphoton laser-scanning lithographic techniques were exploited in the photomediated immobilization of BSA_{488}-*o*NB-CHO over a variety of laser powers (25, 50, 75, 100%) and scan repeats (1, 2, 4, 8, 16). Here, 40 μm x 40 μm square ROIs were scanned at 1 μm z-increments for 50 μm to create an array of protein-functionalized rectangular boxes within the SPAAC-based gels, with each volume corresponding to a unique patterning condition. Samples were imaged using fluorescence confocal microscopy (left), and quantification of immobilized protein concentration (Supplementary Fig. S5) was performed for each light condition (right). Optimal patterning conditions, maximizing total immobilized protein and z-resolution while minimizing patterning speed, were identified as 75% power with 4 scan repeats. Scale bar = 40 μm.

Figure S9 Proteins remain intact upon photorelease

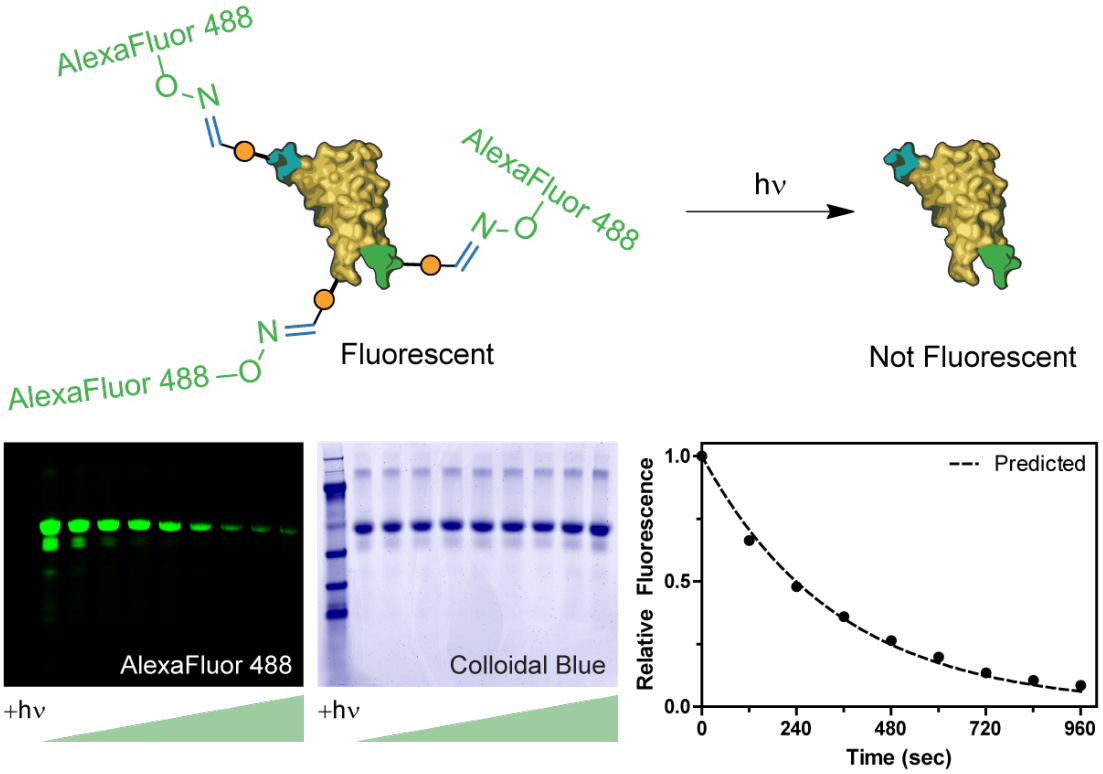

BSA-*o*NB-AF$_{488}$ was dissolved in phosphate-buffered saline (pH = 7.4) at a concentration of 40 μg mL^{-1} and exposed to light (λ = 365 nm, 10 mW cm^{-2}) at room temperature in 2 min increments between 0 and 16 min to induce photocleavage. Proteins and the photoreleased fluorophore (5 μg total) were separated on NuPAGE Novex 4-12% Bis-Tris SDS-PAGE 10-well gels (Life Technologies). Following electrophoresis, gels were imaged for green fluorescence on a GE Typhoon Trio+ scanner (left). Proteins were stained subsequently with Colloidal Blue (Life Technologies) and gels were imaged on the GE Typhoon Trio+ using red-laser excitation of the gel in combination with no emission filter (middle). Relative fluorescence was calculated by normalizing the AlexaFluor 488 signal intensity to that from Colloidal Blue, and compared values predicted on the basis of the photocleavage kinetics of *o*NB-CHO[3] (right).

DOI: 10.1038/NMAT4219

Figure S10 Dose response for photorelease of immobilized proteins

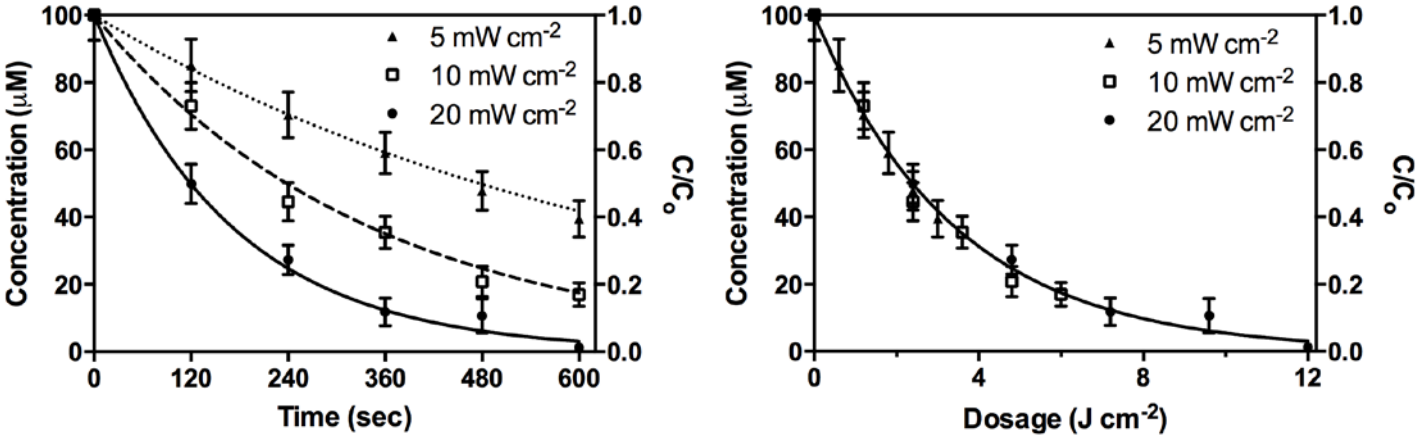

Dose represents the total amount of energy delivered to the system and was calculated as the product of exposure time and light intensity. Connected lines represent predicted protein concentration based on the kinetics of *o*-nitrobenzyl ether (*o*NB) photocleavage[3].

Figure S11 Quantification of 3D protein photoremoval from hydrogel

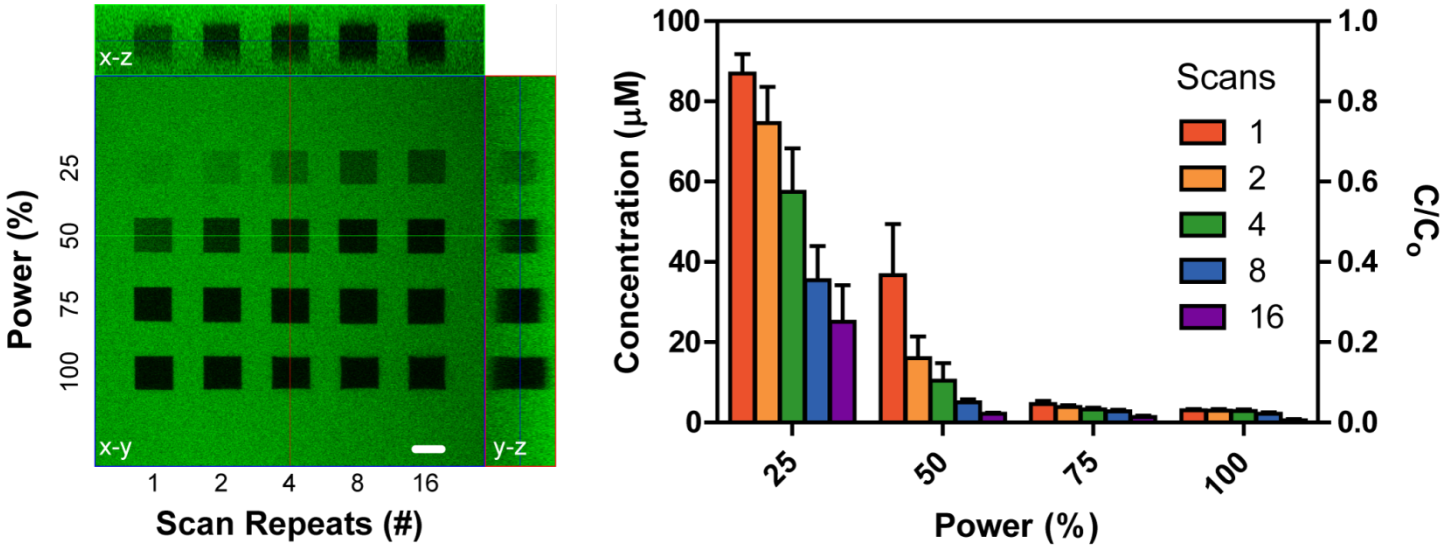

Multiphoton laser-scanning lithographic techniques were exploited to release immobilized BSA_{488}-*o*NB-CHO (initial concentration = 100 μM) over a variety of laser powers (25, 50, 75, 100%) and scan repeats (1, 2, 4, 8, 16). Here, 40 μm x 40 μm square ROIs were scanned at 1 μm z-increments for 50 μm to create an array of protein-depleted rectangular boxes within the SPAAC-based gels, with each volume corresponding to a unique patterning condition. Samples were imaged using fluorescence confocal microscopy (left), and quantification of remaining immobilized protein concentration (Supplementary Fig. S5) was performed for each light condition (right). Optimal patterning conditions, maximizing total protein release and z-resolution while minimizing patterning time, were identified as 50% power with 4 scan repeats. Scale bar = 40 μm.

DOI: 10.1038/NMAT4219

Figure S12 Split color images of photolithographically-generated interconnected protein patterns

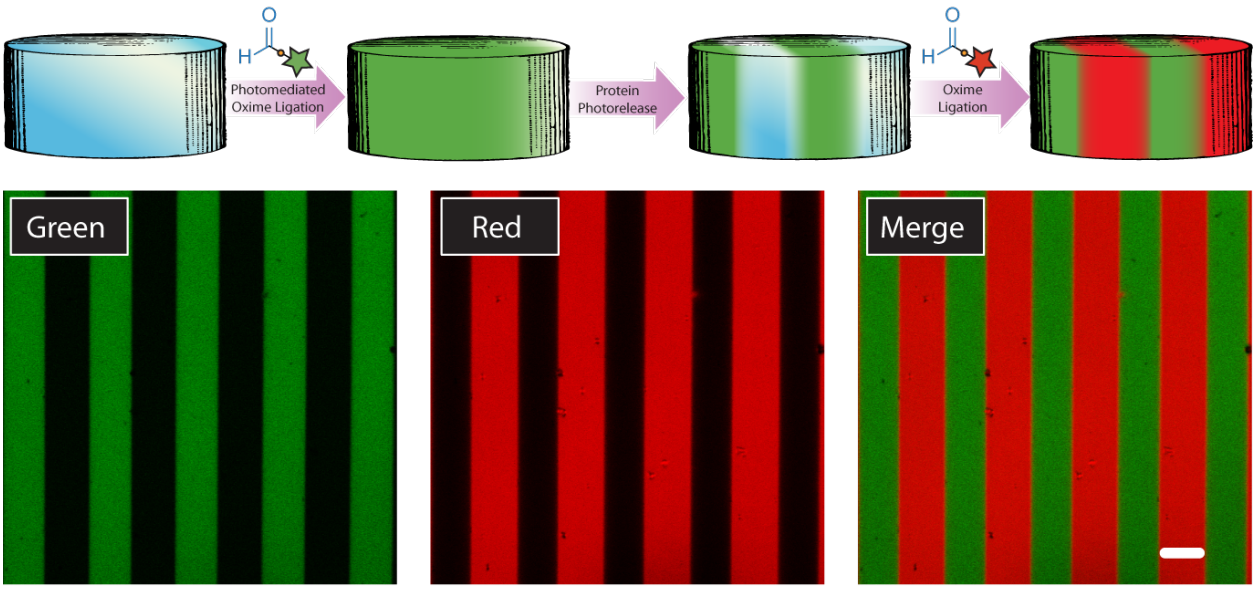

Scale bar = 200 μm.

Figure S13 Split color images of multiphoton laser-scanning lithography-generated interconnected protein patterns (3D)

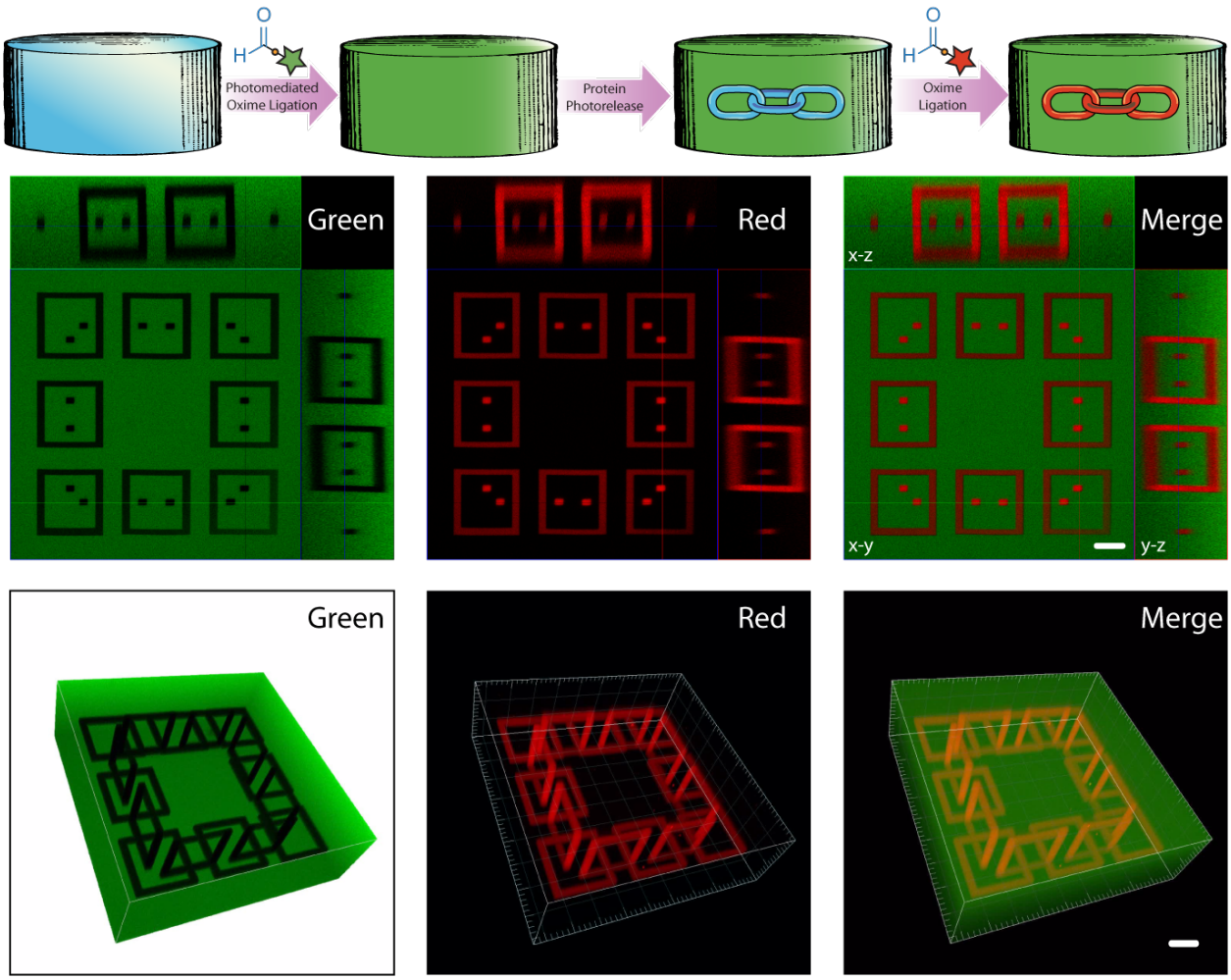

Scale bars = 50 μm.

DOI: 10.1038/NMAT4219

Figure S14 FRAP studies to determine protein diffusion rates in hydrogels

Synthesis of photobleachable fluorescein-labeled BSA ($BSA_{fluorescein}$):
Bovine serum albumin (250 mg, BSA) was dissolved in aqueous sodium bicarbonate (25 mL, 0.1 M, pH = 8.3). Fluorescein-NHS (12.5 mg, Pierce) was dissolved in 100 µL anhydrous dimethylformamide and added to the protein solution. The reaction was allowed to proceed for 2 hr at 25 ºC prior to dialysis (molecular weight cutoff ~ 2 kDa, SpectraPor) and lyophilization. The fluffy yellow product ($BSA_{fluorescein}$) was used with no additional purification. Fluorescein was used to label BSA due to its relatively high susceptibility to photobleaching.

Fluorescence recovery after photobleaching (FRAP) data collection:
$BSA_{fluorescein}$ (100 µM in PBS, pH = 7.4) was swollen into pre-formed hydrogels (1 cm x 2 cm x 100 µm, 10 wt%) for 24 hr at 25 ºC. FRAP experiments were performed on a Zeiss LSM 5 Exciter (Caltech Biological Imaging Center) equipped with a Zeiss Achrostigmat (20x, NA = 0.3) air objective at 25 ºC. A circle (diameter = 50 µm) was bleached within the center of the gel upon repeated scanning (5000 iterations) with the argon laser (λ = 488 nm) at 100% power. Fluorescence recovery was quantified with low laser power (0.5%) iterative scanning (Δt = 0.5 s) over 10 min. To account for photobleaching during FRAP recovery, the mean fluorescence of the bleached spot was normalized to that of an unbleached region of the sample.

FRAP data analysis:
The effective free diffusion (D_f) of $BSA_{fluorescein}$ within the network can be calculated from the simplified diffusion equation[12]:

$$\frac{\partial f}{\partial t} = D_f \nabla^2 f$$

where f is the concentration of free $BSA_{fluorescein}$ as a function of time (t) and ∇^2 is the Laplacian operator. For a circular bleach spot, the closed-form solution involving modified Bessel functions of the first kind (I_0 and I_1) is given by[13]:

$$frap(t) = f(t) = e^{-\frac{\tau_D}{2t}}\left[I_0\left(\frac{\tau_D}{2t}\right) + I_1\left(\frac{\tau_D}{2t}\right)\right]$$

$$\tau_D \equiv \frac{w^2}{D_f}$$

where w is the radius of the bleach spot (25 µm). Fitting experimental FRAP recovery curves using a custom MATLAB script employing the *nlinfit* routine yielded:

$$D_f = 1.8 \text{ x } 10^{-11}\,\frac{\text{m}^2}{s}$$

with a standard deviation of 1.1 x 10^{-12} m s^{-1}. Analogous to what has been observed in similarly-structured PEG networks formed *via* Michael-type addition chemistry[14], this measured coefficient of diffusion is roughly 4 times slower than that of BSA in water[15].

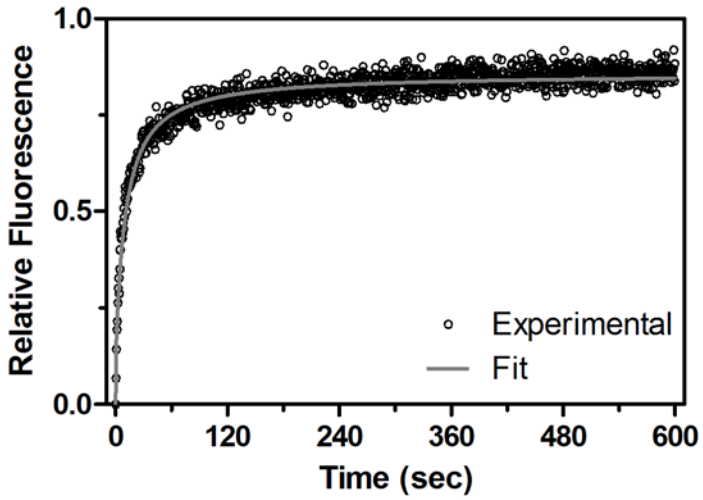

DOI: 10.1038/NMAT4219

Figure S15 Kinetic simulations of protein patterning

To assess the minimum time required to pattern proteins into our hydrogels, we consider the general reaction-diffusion system given by[16]:

$$\frac{\partial C}{\partial t} = D_C \nabla^2 C - r_C$$

where C is the concentration of species C as a function of time (t) and space, D_C is the effective diffusion coefficient, ∇^2 is the Laplacian operator, and r_C is the rate of consumption of species C. Treating the thin, glass-bound hydrogel as an infinite slab of thickness L, we assume a one-dimensional mass transport process with an unchanging bulk concentration of protein in the swelling solution. The second-order, irreversible reaction P + A → O between aldehyde-functionalized protein P and immobilized uncaged alkoxyamine A to form the hydrogel-bound oxime product O proceeds with a rate constant k. For this case, the general reaction-diffusion equation can be simplified for each individual species:

$$\frac{\partial P}{\partial t} = D_P \frac{\partial^2 P}{\partial z^2} - kPA$$

$$\frac{\partial A}{\partial t} = -kPA$$

$$\frac{\partial O}{\partial t} = kPA$$

with initial conditions ($t = 0$):

$$P = 0 \text{ for } 0 \le z \le L$$

$$A = A_0 \text{ for } 0 \le z \le L$$

$$O = 0 \text{ for } 0 \le z \le L$$

subject to boundary conditions ($t > 0$):

$$P = P_\infty \text{ for } z \ge L$$

$$P = 0 \text{ for } z \le 0$$

where A_0 is the initial alkoxyamine A concentration and P_∞ is the bulk concentration of protein P in the swelling solution.

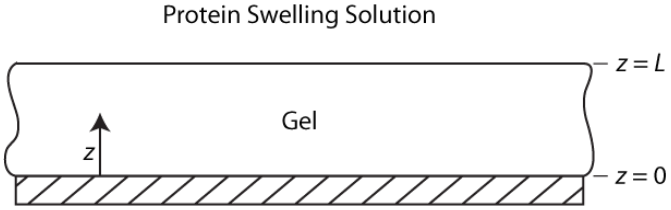

A numerical solution to these coupled partial differential equations based on an explicit Euler finite difference method was implemented with a custom MATLAB script. For a typical gel patterning experiment, we have $k = 10\ M^{-1}\ s^{-1}$ (literature reported value[17]), $D_P = 1.8 \times 10^{-11}\ m^2\ s^{-1}$ (Supplementary Fig. S14), $L = 1000\ \mu m$, $P_\infty = 200\ \mu M$, and $A_0 = 100\ \mu M$ (corresponding to full NPPOC uncaging). Below, we plot the normalized oxime product formation (O/A_0) throughout the gel with time (t):

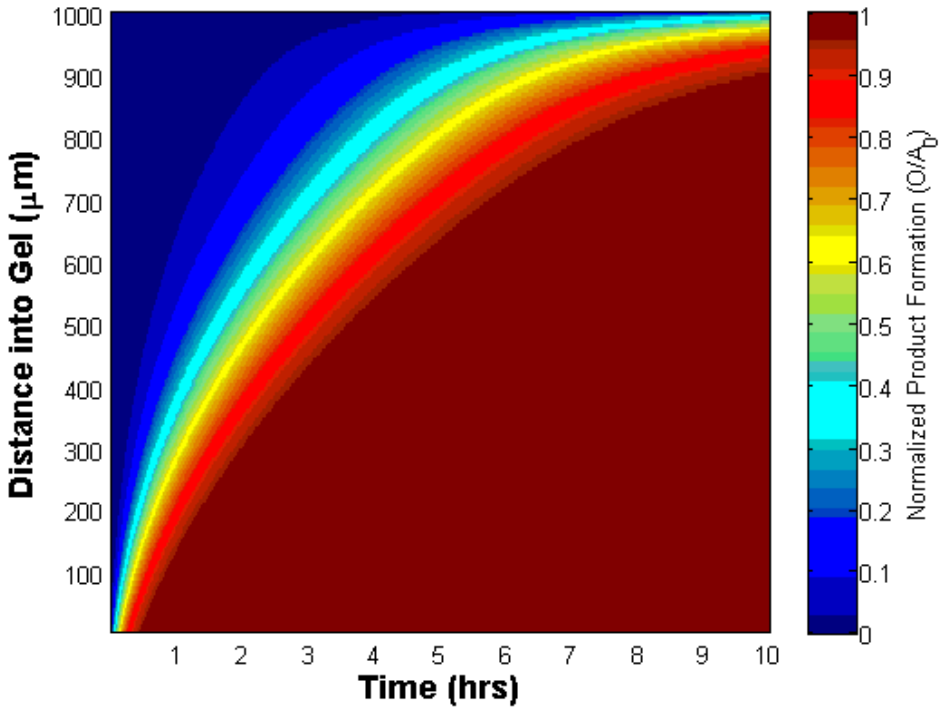

This result indicates that the top 80% of the gel is >90% functionalized after 6.5 hours and that the overnight protein swelling step used in this work is sufficient to achieve full patterning throughout the entirety of the gel. Because the rate of patterning is highly dependent on gel geometry (*i.e.*, sample thickness) and on the nature of the protein (different proteins would be expected to exhibit different diffusion coefficients in the gel), the time at which 90% of the maximum oxime linkages had been formed for all locations ≤ 80% into the material (*i.e.*, $z \leq 0.8L$) was quantified for a variety of thicknesses (L = 100 – 10,000 μm) and diffusion coefficients ($D_P = 0.9 \times 10^{-11}$, 1.8×10^{-11}, and $3.6 \times 10^{-11}\ m^2\ s^{-1}$).

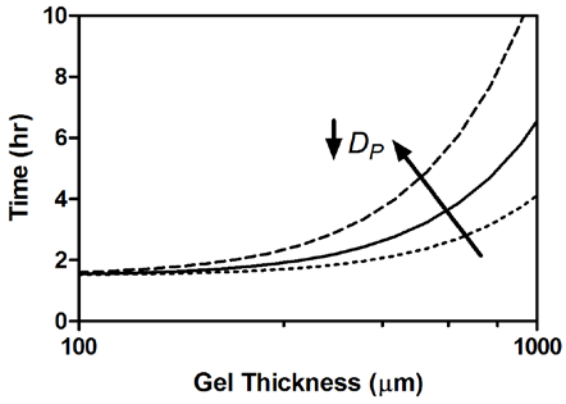

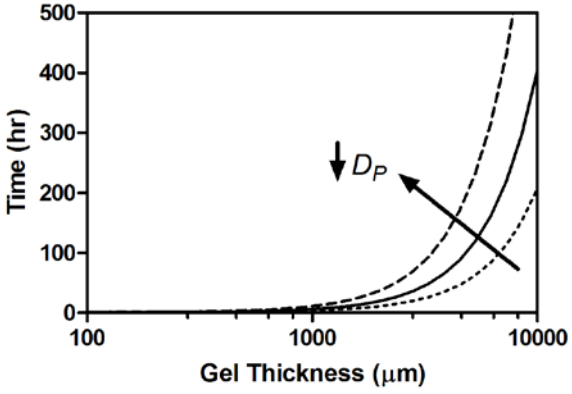

DOI: 10.1038/NMAT4219

These data indicate that the time scale of protein patterning is highly dependent on gel thickness. For relatively thin gels (L ~ 500 μm), patterning is complete after just a few hours (~3 hr). However, this time increases exponentially as thicker gels are considered (~10 days for L ~ 10,000 μm, still assuming an infinite-slab geometry). These calculations provide an estimate of the minimum time required for protein patterning (~1.5 hr), and therefore the time scale over which biological functions can realistically be controlled.

Figure S16 Quantification of enhanced fluorescence for FAM-RGLGPAGRK(FAM)-NH_2 upon collagenase treatment

Phosphate-buffered saline (PBS, pH = 7.4) containing FAM-RGLGPAGRK(FAM)-NH_2 (0.25 mg mL^{-1}, DiFAM, Method S8) and/or collagenase (0.1 mg mL^{-1}, Sigma) was incubated at 37 ^{o}C for 1 hour before quantifying sample fluorescence ($\lambda_{excitation}$ = 494 nm, $\lambda_{emission}$ = 521 nm). An ~8-fold increase in fluorescence was observed upon treatment of FAM-RGLGPAGRK(FAM)-NH_2 with collagenase, corresponding to decreased fluorophore self-quenching upon enzymatic cleavage of the peptide backbone.

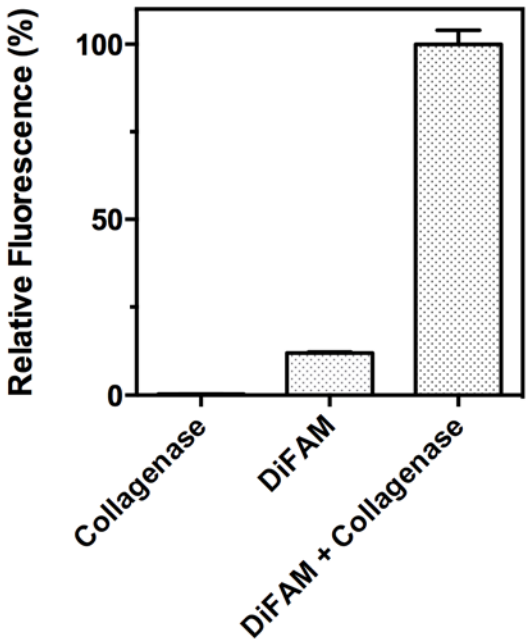

For gel-related studies for Fig. 5a-b, 100 μL cylindrical gels (1 mm thick) were functionalized with collagenase by photomediated oxime ligation and incubated in 900 μL PBS (pH = 7.4) containing DiFAM (final concentration of 0.25 mg mL^{-1}) for 5 hours at 37 ^{o}C with gentle agitation. Solution fluorescence was measured ($\lambda_{excitation}$ = 494 nm, $\lambda_{emission}$ = 521 nm) and used as a measurement of collagenase activity. Additionally, collagenase was photoreleased from the gels into 900 μL PBS. The gel was rinsed with fresh PBS (3x), and then incubated in 900 μL PBS containing DiFAM (final concentration of 0.25 mg mL^{-1}) for 5 hours at 37 ^{o}C prior to measurement of supernatant fluorescence. Finally, 100 μL of PBS containing DiFAM (2.5 mg mL^{-1}) was added to the photoreleased collagenase solution (900 μL), and sample fluorescence was measured after 5 hour incubation at 37 ^{o}C.

DOI: 10.1038/NMAT4219

Figure S17 Quantitative analysis of sustained collagenase bioactivity upon NHS-*o*NB-CHO labeling and photoreversible functionalization

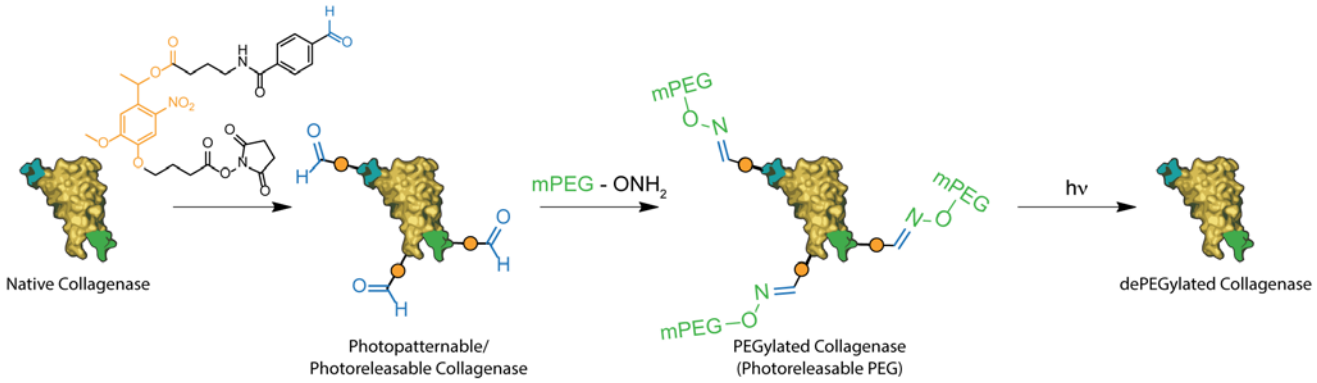

Collagenase-*o*NB-CHO (0.5 mg mL^{-1} in PBS, pH = 7.4, Method S7) was incubated with methoxyPEG-ONH$_2$ (synthesized *via* a known route[18], M_n ~ 5,000 Da, 5 mg mL^{-1}) for 1 hr at 37 ^{o}C to generate the PEGylated enzyme. This PEGylated protein was further exposed to light (λ = 365 nm, 10 mW cm^{-2}, 15 min) at room temperature to induce *o*NB photocleavage and associated dePEGylation. Each protein species (*i.e.*, unmodified collagenase, collagenase-*o*NB-CHO, PEGylated collagenase, and the dePEGylated collagenase) was incubated (0.5 mg mL^{-1} in PBS, pH = 7.4) with FAM-RGLGPAGRK(FAM)-NH$_2$ (0.25 mg/mL, Method S8) at 37 ^{o}C for 1 hour while monitoring real-time changes in sample fluorescence ($\lambda_{excitation}$ = 494 nm, $\lambda_{emission}$ = 521 nm, measurements performed once per minute. A Michaelis-Menten analysis was employed to assess quantitative levels of enzymatic bioactivity following collagenase modification. Experimental progress curves were generated, and the initial slope of the fluorescence versus time plot was taken to be proportional to k_{cat} (substrate concentration = 0.15 mM > K_M ~ 0.01 mM[19]). Relative values for k_{cat} were used to compare enzyme activity for the modified proteins with that of native collagenase. Here, we find that:

$$k_{cat,\ \text{NHS-}o\text{NB-CHO-labeled Collagenase}} = 0.58\ k_{cat,\ \text{Collagenase}}$$
$$k_{cat,\ \text{PEGylated Collagenase}} = 0.24\ k_{cat,\ \text{Collagenase}}$$
$$k_{cat,\ \text{dePEGylated Collagenase}} = 0.47\ k_{cat,\ \text{Collagenase}}$$

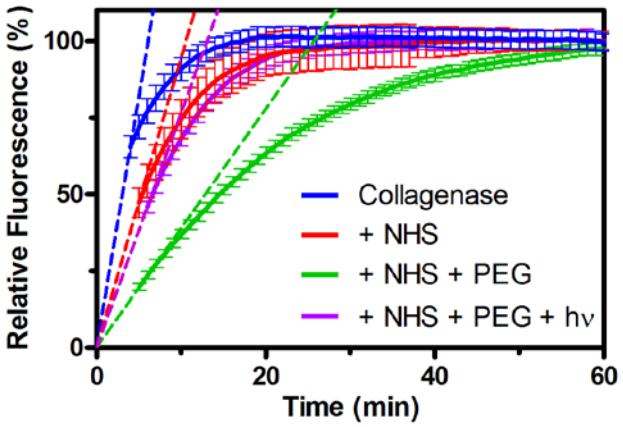

From this, we estimate that collagenase retained ~58% of its original activity upon NHS-*o*NB-CHO labeling, ~24% upon PEGylation, and ~47% upon photomediated dePEGylation.

Figure S18 Controlling hMSC surface attachment with reversibly-patterned vitronectin

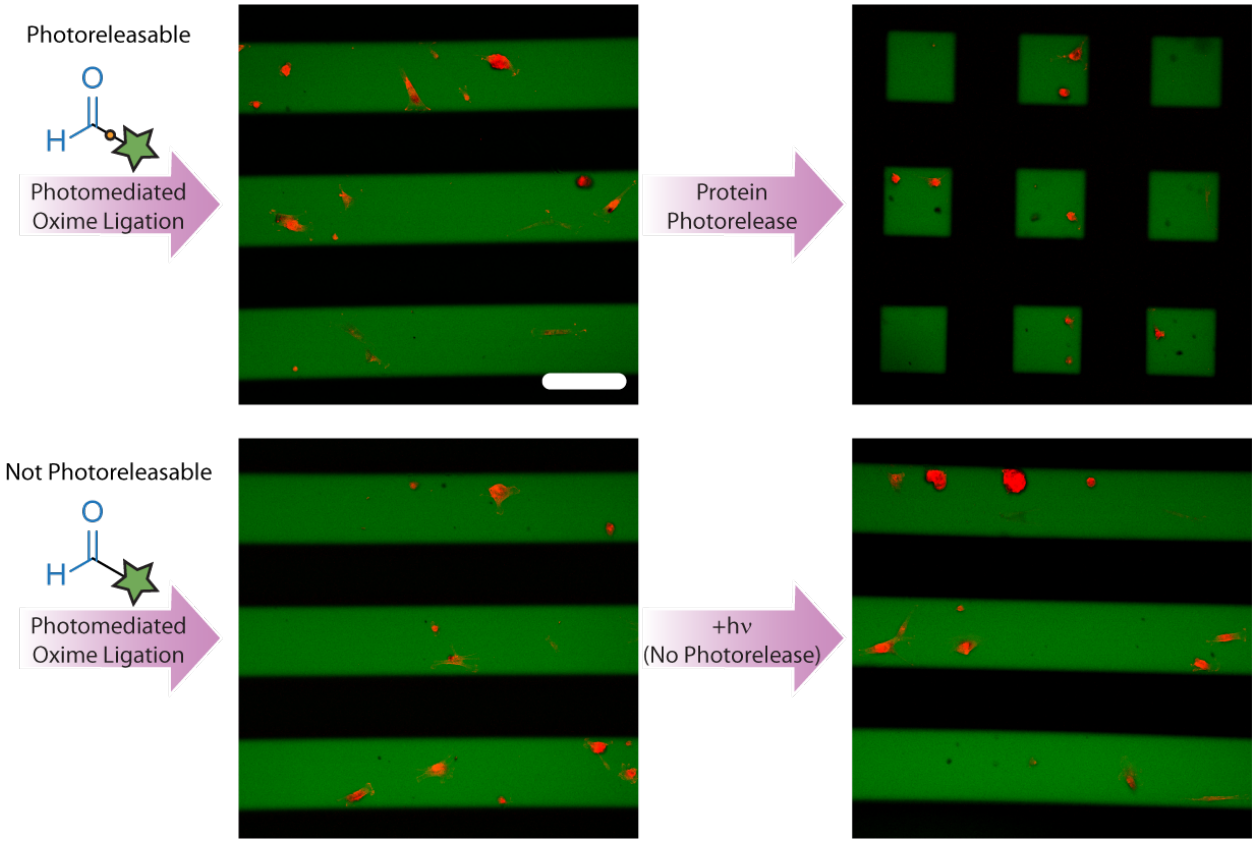

SPAAC-based hydrogels (10 wt%) attached to azide-functionalized glass slides (Supplementary Method S3) were photolithographically-patterned with lines (200 μm wide separated by 200 μm) of either VTN_{488}-*o*NB-CHO (top left, 100 μM) or VTN_{488}-CHO (bottom left, 100 μM) and placed in a untreated 6-well cell culture plate (Corning). hMSCs were seeded onto the patterned gels at 5 x 10^3 cells cm^{-2} (~50 x 10^3 cells suspended in 4 mL fresh media per well, surface area of well bottom = 9.6 cm^2). The gels were rinsed with fresh media 4 hours after seeding to remove non-adherent cells. hMSC attachment and spreading were confined to the VTN-functionalized portions of the material surface (left). 24 hours after seeding, samples were fixed and stained for imaging (see below), and the remaining gels were exposed to collimated UV light (λ = 365 nm, 10 mW cm^{-2}, 15 min) through the same slitted photomask rotated 90º relative to the original pattern. For VTN_{488}-*o*NB-CHO, this procedure transformed the lined pattern into one of 200 μm x 200 μm squares (top right), causing localized hMSC detachment in regions of protein photorelease. The VTN_{488}-CHO pattern was unaltered by the light exposure (bottom right), and cells remained attached to the original line patterns. Vitronectin is shown in green, F-actin is shown in red. Scale bar = 200 μm.

Staining for F-actin

24 hours after seeding, or 4 hours after vitronectin protein photorelease, hydrogels were washed twice with phosphate-buffered saline (PBS, pH = 7.4) and fixed in paraformaldehyde (3.7% in PBS) for 15 min at 25 ºC. Cell membranes were permeabilized over 5 min with Triton® X-100 (0.5% in PBS). Samples were blocked with BSA (3% in PBS) for 30 min prior to staining with

DOI: 10.1038/NMAT4219

AlexaFluor 594 phalloidin (5 U mL^{-1} PBS, Invitrogen). After incubation (1 hr), the samples were washed with PBS and visualized using fluorescence confocal microscopy.

Figure S19 Viability of hMSCs in photopatterned hydrogels

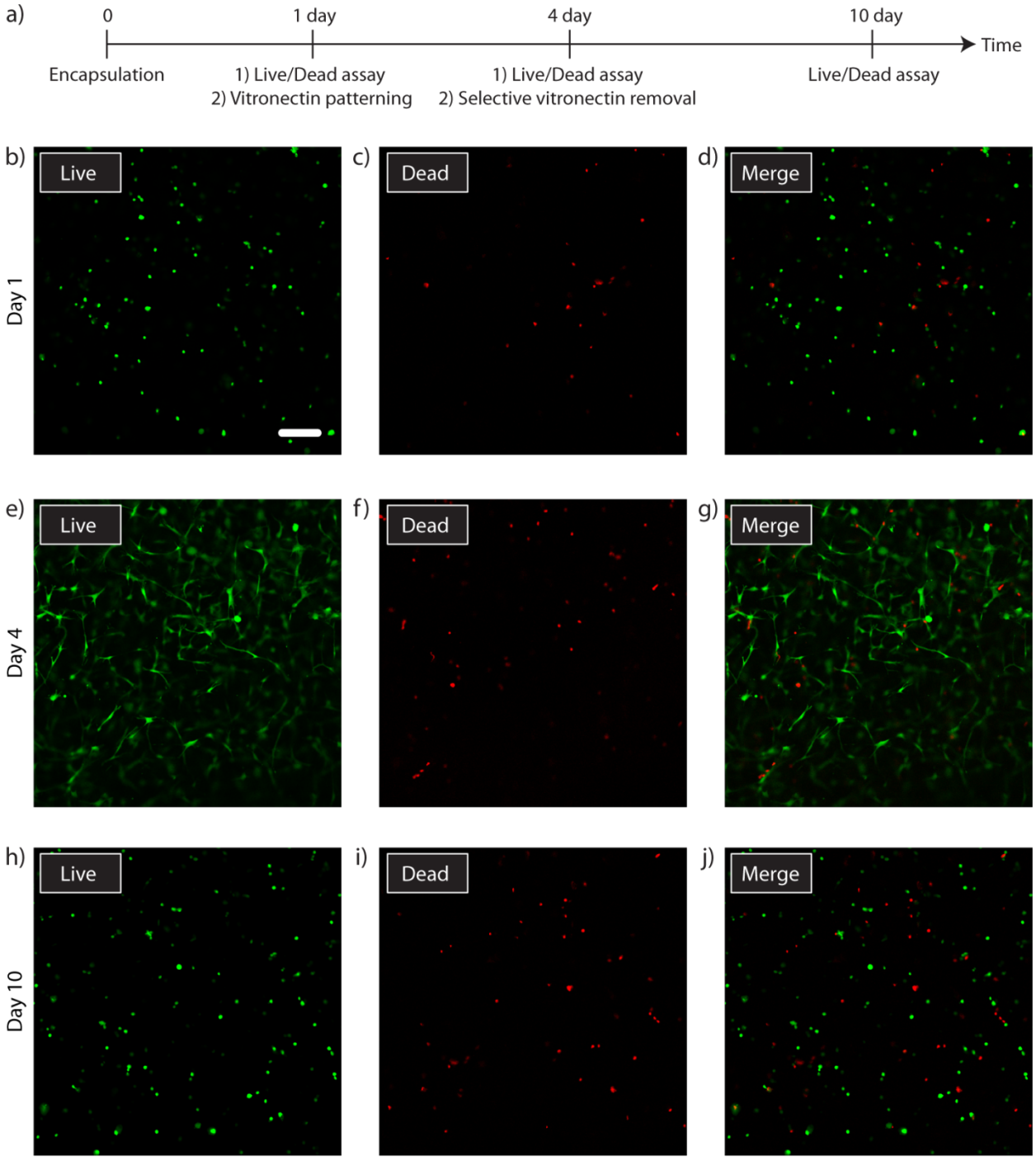

Day 0 – Human mesenchymal stem cells (hMSCs, passage 3) were encapsulated in 10 wt% SPAAC-based hydrogels in PBS at a density of 3 x 10^6 cells mL^{-1}. After 30 min, the gels were transferred to osteogenic media and incubated in 5% CO_2 at 37 °C.

Day 1 – A subset of the cell-laden gels was stained with a Live/Dead assay (Invitrogen) and visualized with fluorescence confocal microscopy. High viability (~90%) was observed. The

DOI: 10.1038/NMAT4219

unstained hydrogels were uniformly irradiated (5 min) with collimated UV light (λ = 365 nm, 20 mW cm^{-2}) and swollen in osteogenic media containing VTN-*o*NB-CHO (100 μM) overnight. Unreacted protein was removed by swelling into fresh media, yielding a VTN-modified hydrogel.

Day 4 – A subset of the cell-laden, VTN-*o*NB-CHO-labeled gels was subjected to a Live/Dead assay (Invitrogen) and visualized with fluorescence confocal microscopy. High viability post-encapsulation and photo-mediated protein immobilization (~85%) was observed. Unstained gels, previously patterned with VTN-*o*NB-CHO, were uniformly irradiated (5 min, λ = 365 nm, 20 mW cm^{-2}) before being returned to osteogenic media.

Day 10 – Remaining samples were analyzed by Live/Dead assay (Invitrogen) and fluorescence confocal microscopy. Though a significant portion of the cells remained viable (~70%), this is consistent with other reports indicating that attachment may be required for long-term survival of hMSCs within synthetic hydrogels.

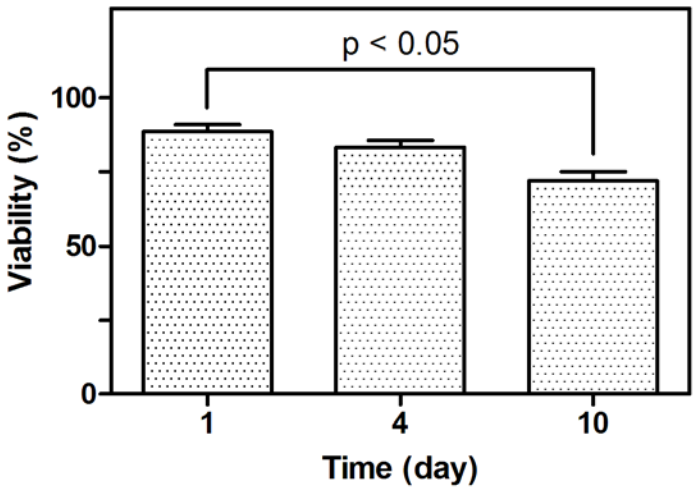

Movie S1 **3D protein pattern generated *via* photomediated oxime ligation**

Movie S2 **Altered 3D protein pattern generated *via* *o*-nitrobenzyl ether linker photocleavage**

Movie S3 **3D interconnected dual-protein pattern generated through multiphoton-based protein photorelease and oxime ligation**

Movie S4 **3D spatial and temporal control of hMSC differentiation by photoreversible patterning of vitronectin**

DOI: 10.1038/NMAT4219

References

1. Still, W.C., Kahn, M. & Mitra, A. Rapid Chromatographic Technique for Preparative Separations with Moderate Resolution. *J. Org. Chem.* **43**, 2923-2925 (1978).
2. Dommerholt, J. et al. Readily Accessible Bicyclononynes for Bioorthogonal Labeling and Three-Dimensional Imaging of Living Cells. *Angew. Chem. Int. Ed. Engl.* **49**, 9422-9425 (2010).
3. DeForest, C.A. & Anseth, K.S. Cytocompatible click-based hydrogels with dynamically tunable properties through orthogonal photocoupling and photodegradation reactions. *Nat. Chem.* **3**, 925-931 (2011).
4. Godula, K., Rabuka, D., Nam, K.T. & Bertozzi, C.R. Synthesis and microcontact printing of dual end-functionalized mucin-like glycopolymers for microarray applications. *Angew. Chem. Int. Ed. Engl.* **48**, 4973-4976 (2009).
5. Walba, D.M. et al. Self-assembled monolayers for liquid crystal alignment: simple preparation on glass using alkyltrialkoxysilanes. *Liquid Crystals* **31**, 481-489 (2004).
6. Kim, C.H. et al. Synthesis of Bispecific Antibodies using Genetically Encoded Unnatural Amino Acids. *J. Am. Chem. Soc.* **134**, 9918-9921 (2012).
7. Mancini, R.J., Li, R.C., Tolstyka, Z.P. & Maynard, H.D. Synthesis of a photo-caged aminooxy alkane thiol. *Org. Biomol. Chem.* **7**, 4954-4959 (2009).
8. Phillips, J.A. et al. Single-Step Conjugation of Bioactive Peptides to Proteins via a Self-Contained Succinimidyl Bis-Arylhydrazone. *Bioconjug. Chem.* **20**, 1950-1957 (2009).
9. Odian, G.G. Principles of polymerization, Edn. 4th. (Wiley-Interscience, Hoboken, N.J.; 2004).
10. Invitrogen. Amine-Reactive Probes. (2011).
11. Johnson, P.M., Reynolds, T.B., Stansbury, J.W. & Bowman, C.N. High throughput kinetic analysis of photopolymer conversion using composition and exposure time gradients. *Polymer* **46**, 3300-3306 (2005).
12. Sprague, B.L., Pego, R.L., Stavreva, D.A. & McNally, J.G. Analysis of binding reactions by fluorescence recovery after photobleaching. *Biophys. J.* **86**, 3473-3495 (2004).
13. Soumpasis, D.M. Theoretical analysis of fluorescence photobleaching recovery experiments. *Biophys. J.* **41**, 95-97 (1983).
14. Zustiak, S.P. & Leach, J.B. Characterization of protein release from hydrolytically degradable poly(ethylene glycol) hydrogels. *Biotechnol. Bioeng.* **108**, 197-206 (2011).
15. Phillies, G.D. Diffusion of bovine serum albumin in a neutral polymer solution. *Biopolymers* **24**, 379-386 (1985).
16. Fogler, H.S. Elements of chemical reaction engineering, Edn. 4th. (Prentice Hall PTR, Upper Saddle River, NJ; 2006).
17. Blanden, A.R., Mukherjee, K., Dilek, O., Loew, M. & Bane, S.L. 4-Aminophenylalanine as a Biocompatible Nucleophilic Catalyst for Hydrazone Ligations at Low Temperature and Neutral pH. *Bioconjug. Chem.* **22**, 1954-1961 (2011).
18. Carrico, I.S., Carlson, B.L. & Bertozzi, C.R. Introducing genetically encoded aldehydes into proteins. *Nat. Chem. Biol.* **3**, 321-322 (2007).
19. Marokhazi, J. et al. Enzymic characterization with progress curve analysis of a collagen peptidase from an enthomopathogenic bacterium, Photorhabdus luminescens. *Biochem. J.* **379**, 633-640 (2004).